Physical Features

1.1 Introduction

Physical oceanographic data provide invaluable insight on the understanding of ocean circulation and changes in the horizontal and vertical distribution of sea properties/parameters also in response to natural and man-induced changes, such as climate change, land-based discharges into the sea as well as other activities that can alter such parameters, which in turn may affect water quality and marine species and habitats.

This Chapter provides information on the topography, bathymetry, general circulation and the climatological characteristics of water masses in the south-central Mediterranean, since the hydrodynamics of the upper layer in the area of the Maltese Islands is mainly dictated by the general flow in the Sicilian Channel.

The first physical oceanographic campaign in Malta (focused on the north western coastal area), was undertaken in 1992 by the Physical Oceanography Unit (PO Unit – University of Malta). Since then significant advancements have been made in this field and which have combined *in situ* hydrographic observations with numerical modelling simulations and satellite imagery. Major works to study sea circulation *inter alia* include Drago (1997) [1], Drago and Sorgente (2001)[2], Drago *et al.* (2003)[3], Sorgente *et al.* (2003)[4], and Drago *et al.* (2010)[5]. The modelling approach that has been mainly applied is a primitive equation numerical model, based on the Princeton Ocean Model (POM)[6]. The information provided on physical features in sections 1.2, 1.3, 1.4, 1.5 and 1.7 in this Chapter originates mainly from these works. Supporting data at the sub-basin scale are also obtained online and are generated by the Operational Oceanography Group (G3O) of the Institute for the Marine and Coastal Environment - National Research Council (IAMC-CNR) [7] of Oristano and MyOcean.

This Chapter also builds on information extracted from a number of commissioned studies such as on the analysis of hydrodynamics (Alpha Briggs, 2008), the assessment of significant wave heights by Scott Wilson Kirkpatrick and Co. Ltd (2003), and the monitoring of physicochemical parameters under the Water Framework Directive (CIBM and Ambiente SC, 2013) and Bathing Water Quality Directive.

---

1 Drago, A.F. 1997. Hydrographic Measurements in the North Western Coastal Area of Malta. *Xjenza, Journal of the Malta Chamber of Scientists 2*, 1, 6-14.

2 Drago, A.F. and Sorgente R. (2001). A One Nested High Resolution Circulation Model in the Malta Channel. *Rapp. Comm. int. Mer Médit., 36: 58p.*

3 Drago, A.F., Sorgente, R., and Ribotti, A. (2003). A high resolution hydrodynamical 3D model of the Malta Shelf area. In *Annales Geophysicae*, 21: 323-344 pp.

4 Sorgente, R., Drago, A. and Ribotti, A. (2003). Seasonal variability in the Central Mediterranean Sea circulation. *Annales Geophysicae*, 21, 299 - 322.

5 Drago, A., Sorgente, R., and Olita, A. (2010). Sea temperature, salinity and total velocity climatological fields for the south-central Mediterranean Sea. GCP/RER/010/ITA/MSM-TD-14. *MedSudMed Technical Documents*, 14: 35 pp.

6 The model runs with full atmospheric forcing and includes complete thermohaline dynamics. The model runs on a hierarchy of embedded models linking in a one-way offline nesting mode to the basin scale Mediterranean Ocean General Circulation Model from which analysis fields are used. The numerical model output is expressed as a time series of daily averaged currents, temperature and salinity fields.

7 http://www.seaforecast.cnr.it/forecast/en

1.2 Topography and bathymetry of the seabed

Topography and bathymetry, which are used to describe bottom contours of the seabed, both influence the flow of water in an area as the moving water interacts with the ocean floor. This then has direct implications on the bottom substrate characteristics and hence on aquatic habitats, including fish populations. Changes in sea depth also lead to variations in temperature, salinity and nutrient concentrations, and finally dictate which species live there.

The topography and bathymetry of the Maltese Islands, as documented in the work of Drago *et al*. (2010)[8], influence the flow of water in the central area of the Strait of Sicily Figure 1. The latter corresponds to the narrow passageway connecting the western and eastern Mediterranean sub-basins and is characterised by a complex bathymetry with wide continental shelves, deep and shallow channels as well as wide abyssal plains. It plays a crucial role in the passage of the superficial and intermediate water masses in transit between the eastern and the western Mediterranean sub-basins and also prevents the direct mixing of the water masses from the deep and bottom layers of the two sub-basins.

[8] Drago, A., Sorgente, R., and Olita, A. (2010). Sea temperature, salinity and total velocity climatological fields for the south-central Mediterranean Sea. GCP/RER/010/ITA/MSM-TD-14. *MedSudMed Technical Documents*, 14: 35 pp.

Figure 1: The bathymetry, in metres, of the Straits of Sicily shown in grey contours, from light (shallow) to dark (deep)[9]

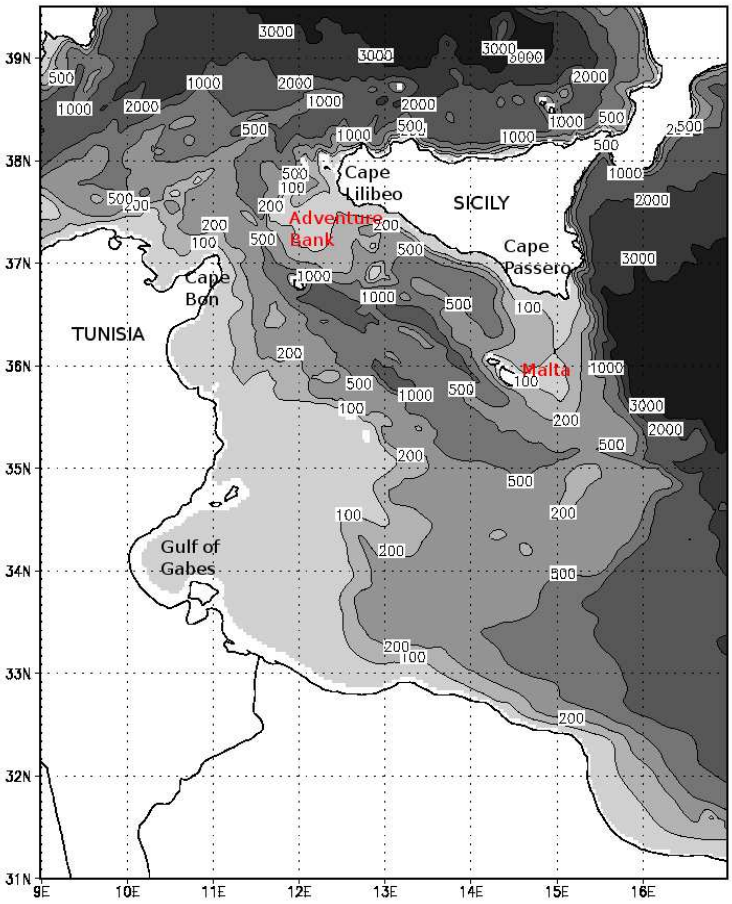

As seen in Figure 1, the strait between Cape Bon (Tunisia) and Cape Lilibeo (Sicily) is the narrowest constriction (1243km wide) and constitutes the main exchange passageway for the superficial and intermediate water masses between the two sub-basins. The flow is further limited by the highly irregular bottom topography. The Maltese Archipelago, aligned in a NW-SE direction, is located on the southernmost extremity of the Malta platform. The topography of the continental shelf in this area is characterised by a plateau in the middle part, with an average depth of 150 m. The shelf is flanked by a submarine ridge, which protrudes as a submerged extension of Cape Passero and embraces the shelf area along the eastern and southern perimeter. The Maltese Islands represent the emerged part of this ridge while Hurd Bank to the north east of Malta shallows to a depth of just over 50 m. Figure 2 gives a three-dimensional view of the bottom relief around the Maltese Islands as seen from the west.

[9] Extracted from: Drago, A., Sorgente, R., and Olita, A. (2010). Sea temperature, salinity and total velocity climatological fields for the south-central Mediterranean Sea. GCP/RER/010/ITA/MSM-TD-14. *MedSudMed Technical Documents*, 14: 35 pp.

Figure 2: 3-D view of the model bathymetry[10]

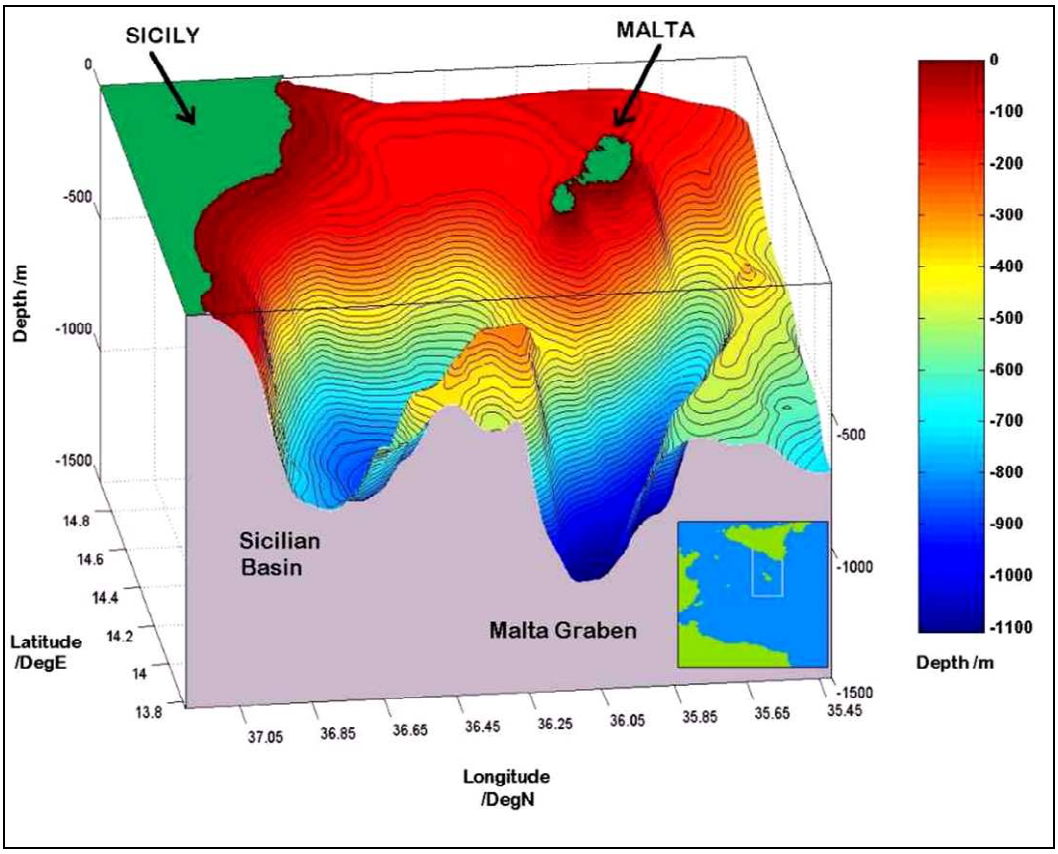

To the southeast a series of relatively shallow areas, notably the Medina Bank (Point vi in Figure 3 below), maintain an average depth of less than 300 m. On the southern coast of Sicily the shelf is bounded by two wide (approx. 100 Km) and shallow (100 m) banks on the western (Adventure Bank – Point iii in Figure 3) and eastern extremities (Malta Channel area – Point iv in Figure 3), while it narrows down considerably along its middle part. The shelf is interrupted from its extension towards the west by the relatively deep Gela Sicilian basin (Figure 2) separating it from Adventure Bank. On its eastern extremity, it deepens abruptly into the deep Ionian Sea with a very sharp escarpment (known as the Malta Escarpment). The Malta Trough (referred to as 'Malta Graben' in Figure 2) to the south west of Malta forms part of a cluster of flat bottomed depressions reaching a depth of around 1650m. The islands are very close to the shelf break and flanked by a very steep bathymetry in the south[11].

Figure 3: Topography and Bathymetry of the Strait of Sicily region

[10] Extracted from: Drago, A.F., Sorgente, R., and Ribotti, A. (2003). A high resolution hydrodynamical 3D model of the Malta Shelf area. In *Annales Geophysicae*, 21: 323-344 pp.

[11] Drago A. (2003). *Addressing the need of marine observations for fisheries*. In: Proceedings of the Fourth APS Annual Seminar on the Development of Agriculture and Fisheries in Malta. 33-73pp.

The numbers indicate Pantelleria Island (1), Maltese Islands (2), Sicily (3), Tunisia (4) and Calabria (5). The (i)'s indicate topographic features: the Ionian slope (i), Tunisian shelf (ii), Adventure Bank (iii), Maltese plateau (iv), Messina Rise (v) and Medina Bank (vi).
Source: Lermusiaux & Robinson (2001)

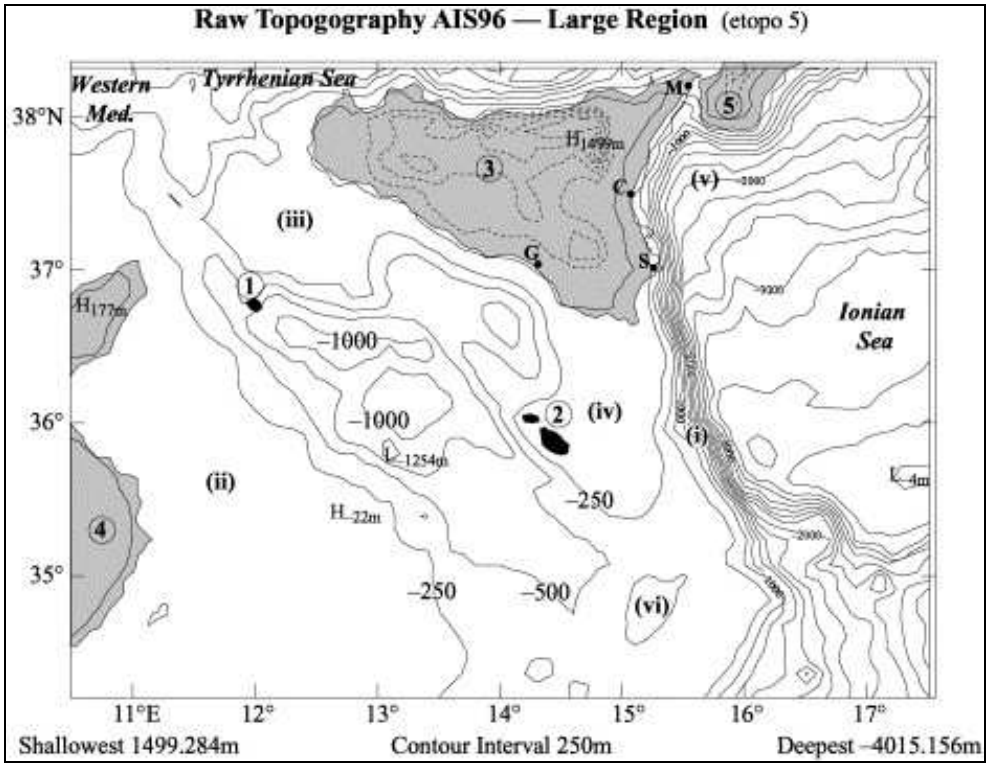

On a more local scale, information on geomorphology and substrate types pertains mainly to coastal waters. Past surveys[12] imply that, in general, the Northeastern coast of the Maltese Islands is characterised by a gently sloping shore which continues underwater as a gently sloping rocky bottom. Further offshore a change in seabed type from rock to sand occurs. The latter substratum is generally highly heterogenous and may be characterised by a mosaic of substrata, which apart from bare sand would include sand intermixed with cobbles/pebbles/shingle, small boulders and patches of bedrock covered by a thin layer of sand. In contrast most of the Southwestern coast of the Maltese Islands is characterised by cliffs and boulder screes. Studies focusing on two sites within this area[13] indicate that the seabed adjacent to the coastline within these sites is characterised by vertical drop-offs with boulder fields at their base.

[12] Borg, J.A.; Micallef, S.A.; Pirotta, K. & Schembri, P.J. 1997. Baseline Marine Benthic Surveys in the Maltese Islands (Central Mediterranean). In: Ozhan, E. (Ed.) *Proceedings of the Third International Conference on the Mediterranean Coastal Environment, MEDCOAST 97, November 11-14, 1997; Qawra, Malta*

[13] Borg, J.A.; Micallef, S.A.; Pirotta, K. & Schembri, P.J. 1997. Baseline Marine Benthic Surveys in the Maltese Islands (Central Mediterranean). In: Ozhan, E. (Ed.) *Proceedings of the Third International Conference on the Mediterranean Coastal Environment, MEDCOAST 97, November 11-14, 1997; Qawra, Malta*

The geology and morphology of the seabed within an area extending from offshore north Gozo to south-east Malta were recently investigated by Micallef *et al*. (2013)[14]. The study area covers the bathymetric depth range of 5–250m and is mainly characterised by flat to gently sloping seafloor. A steep escarpment at a depth of 120–130 m divides the seafloor into two parts:

(i) the 'shallow' part, at depths less than 45 m is mostly covered by *Posidonia oceanica* meadows colonising both coarse grained sediment and bedrock. At greater depths, this part is mainly characterised by maerl associated with sand and gravel, however it also comprises areas characterised by medium-fine sands.

(ii) the 'deeper' part of the seafloor is a smooth, featureless surface almost entirely composed of medium to fine sand.

Overall, the least extensive natural seafloor composition class is unvegetated bedrock. The distribution of substrate types as plotted through this survey is being reproduced in Figure 4.

Figure 4: Distribution of different substrate types as recorded by Micallef *et al*. (2013)[15]

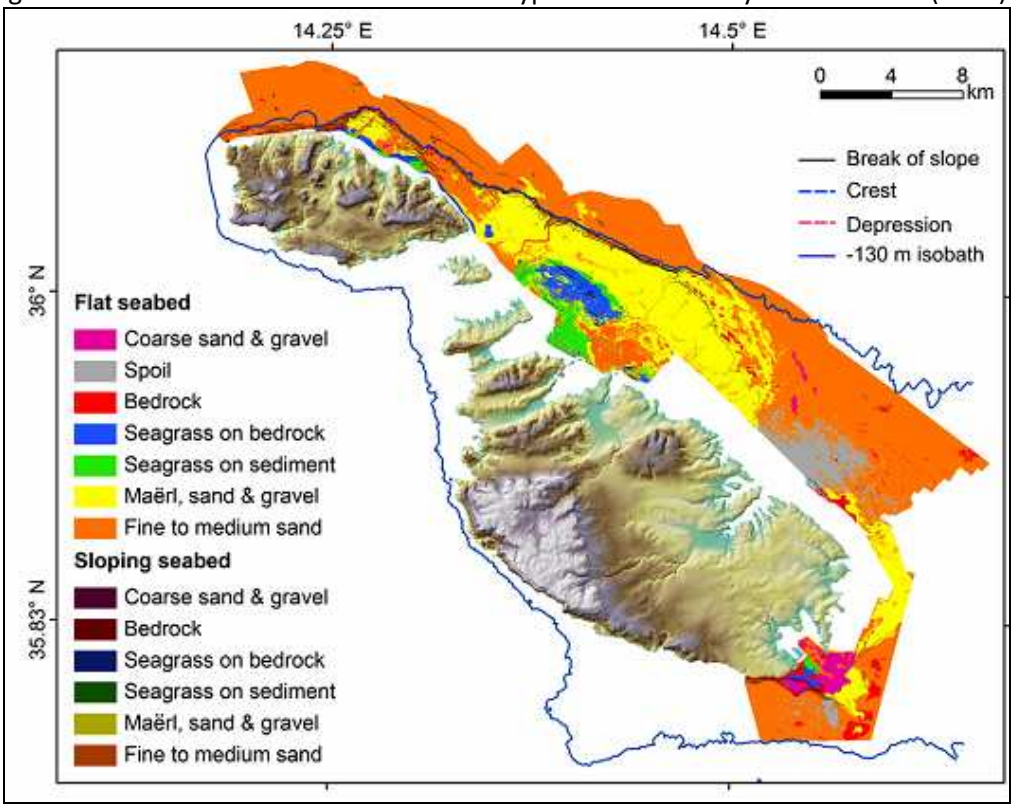

[14] Micallef, A.; Foglini, F.; LeBas, T.; Angeletti, L.; Maselli, V.; Pasuto, A. & Taviani, M. 2013. The submerged paleolandscape of the Maltese Islands: Morphology, evolution and relation to Quaternary environmental change. *Marine Geology*. 335: 129-147

[15] Micallef, A.; Foglini, F.; LeBas, T.; Angeletti, L.; Maselli, V.; Pasuto, A. & Taviani, M. 2013. The submerged paleolandscape of the Maltese Islands: Morphology, evolution and relation to Quaternary environmental change. *Marine Geology*. 335: 129-147

In addition, a Bathymetric LiDAR Scan and a Bathymetric Acoustic Scan were carried out from May – June 2012 and April - November 2012 respectively within 1 nautical mile of marine waters as part of the ERDF 156: *Development of Environmental Monitoring Strategy and Environmental Monitoring Baseline Surveys*. Nevertheless, the final data sets were not available at the time of compilation of this report.

1.2 Circulation, Water Mixing Characteristics and Residence Time

The information presented here on the circulation and the water column structure in the Central Mediterranean Sea is on the basis of information documented by Drago *et al.* (2010)[16] unless otherwise stated. The general circulation is mainly driven by the slow Mediterranean thermohaline circulation, together with its mesoscale[17] and seasonal variability (Figure 5). This leads to the formation of a vertical structure of the water masses described hereunder[18, 19].

Figure 5: Schematic of circulation in the Strait of Sicily according to Astraldi, Gasparini and Gervasio (2001)[20] and Lermusiaux and Robinson (2001)[21]

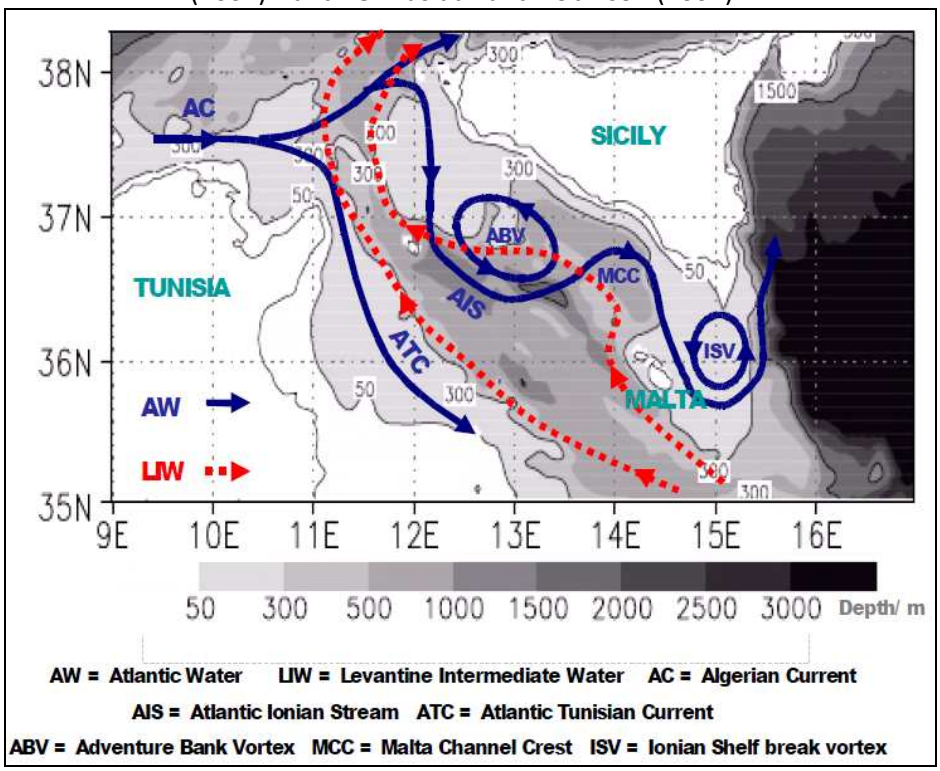

[16] Drago, A., Sorgente, R., and Olita, A. (2010). Sea temperature, salinity and total velocity climatological fields for the south-central Mediterranean Sea. GCP/RER/010/ITA/MSM-TD-14. *MedSudMed Technical Documents*, 14: 35 pp.

[17] Mesoscale features include the cyclonic Adventure Bank Vortex (ABV), the anticyclonic Maltese Channel Crest (MCC), the cyclonic Ionian shelf Break Vortex (ISV) and the intermittent cyclonic Messina Rise Vortex (see Figure 3).

[18] Robinson *et al*. (1996) have identified seven water masses in the northern area of the Strait of Sicily and the northwest Ionian Sea. Starting from the Modified Levantine Intermediate Water (MLIW) at the bottom, the successive overlying layers consist of the Transitional, Fresh, Mixed, Modified Atlantic, Upper and Surface water masses.

[19] Warn-Vargas, A., Sellschopp, J., Haley Jr. P.J., Leslie, W.G., and Lozano, C.J. (1999). Strait of Sicily water masses. *Dyn. Atmos. Oceans*, **29**: 437-469 pp.

[20] Astraldi, M., Gasparini, G.P. and Gervasio, L. (2001). Dense Water Dynamics along the Strait of Sicily (Mediterranean Sea) *Journal of Physical Oceanography*, 31: 3457-3475pp.

[21] Source: Drago, A., Sorgente, R., and Olita, A. (2010). Sea temperature, salinity and total velocity climatological fields for the south-central Mediterranean Sea. GCP/RER/010/ITA/MSM-TD-14. *MedSudMed Technical Documents*, 14: 35 pp.

Surface Circulation

Modified Atlantic Water: The upper water mass (up to 100m depth) consists of cooler and less saline (T= 15 to 17°C; S = 37.2 to 37.8) Modified Atlantic Water (MAW), which is directed eastward and is transported by the Algerian Current (AC). The latter unstable coastal boundary current is subject to significant mesoscale variability and a complex surface pattern due to the bottom topography. The MAW is a broad homogeneous layer that undergoes progressive modifications becoming warmer and saltier as it spreads toward the eastern Mediterranean basin. The MAW, on approaching the Straits of Sicily splits in two branches: the branch that passes the region of the Straits of Sicily constitutes the energetic and meandering Atlantic Ionian Stream (AIS), while the southern branch is called the Atlantic Tunisian Current (ATC) and flows along the Tunisian shelf break. Both branches are characterised by a strong seasonal variability, in terms of path and hydrological features. The AIS circulation represents the main flow of the surface MAW and has a characteristic lower sub-surface temperature, which leads to changes in SST as it undergoes large scale movements with the associated vertical mixing. Its path starts as a meander to the south of the Adventure Bank, proceeding south eastwards and looping back to the north around Malta, forming the Malta Channel Crest (MCC in Figure 5). In particular, during summer and autumn, the flow takes the consistency of a jet stream, gaining abruptly positive vorticity as it reaches the sharp shelf break to the east of Malta, and tending to deflect northward with an intense looping meander, forming the characteristic Ionian Shelf Break Vortex (ISV in Figure 5). The upshooting of the AIS follows closely the Ionian shelf break and subsequently extends as a relatively strong velocity front into the north western Ionian, where the circulation is predominantly anticyclonic. The MAW vein close to the southern Sicilian coast is most conspicuous during summer and autumn, proceeding eastward along the swift topographically controlled AIS. During winter, the MAW fills the whole extent of the Strait up to the westernmost tip of the southern Sicilian shelf. Starting from spring, this MAW then starts to progressively detach from the surface, taking the form of a subsurface core at a depth of about 60m in autumn.

Ionian Water: The layer of Ionian Water (IW; T= 15 to 16.5 °C, S = 37.8 to 38.4) resides as a subsurface layer (50-100 m depth) in the eastern extremity of the area, mainly south of Malta on the Malta shelf areas.

Intermediate and Deeper Water Circulation

Levantine Intermediate Water: The layer (at an average depth of 200 to 280m) of more saline Modified Levantine Intermediate Water (MLIW; T = 13.75 to 13.92 °C and S = 38.73 to 38.78 at the Straits of Sicily) moves in the opposite direction towards the west. The LIW is formed mainly in the north eastern Levantine basin during winter as a result of cooling and evaporation processes and then it spreads westward at an intermediate depth, penetrating over the Central Mediterranean ridge and eventually entering the western basin after crossing the Strait of Sicily. The LIW enters the Sicily Channel through the Medina sill to the southeast of Malta where the sea bottom rises from a depth of over 2000m to a mean of

around 400 m with a salinity of about 38.74 to 38.75 psu and a temperature of about 14.0 to 14.1°C in autumn-winter. In the Sicilian Channel the LIW stream is strongly controlled by the topography. The morphology obliges the LIW to pass along the southern proximity of Malta and to subsequently spread again as it reaches the flanks of Adventure Bank. The flux of LIW is not constant but subject to a seasonal variability and calculated to be 2–3 times higher in winter with respect to summer. The thickness of the LIW layer changes substantially with the seasons, wider in fall-winter and thicker in spring-summer. Its core depth varies seasonally with the LIW being deeper in winter, below 200 m, and closer to the surface in summer and autumn. The renewal time of the total LIW in the Straits of Sicily is estimated to be 9 months, long enough to maintain fairly constant salinity over the annual cycle. This also indicates that the characteristics of the LIW incident in the Straits of Sicily from the eastern Mediterranean are also quite stable. The LIW can be identified by the relative maximum in temperature and an absolute maximum in salinity at an intermediate depth, between about 200 and 600 m in the Straits of Sicily.

Eastern Overflow Water: The deeper Eastern Overflow Water (EOW) represents the water incident from the eastern Mediterranean overflowing over the south–central Mediterranean ridge into the Tyrrhenian Sea. It consists of LIW and Eastern Mediterranean Deep Water (EMDW) which is colder and fresher than the LIW. Below the LIW there is a significant volume of transient EMDW (tEMDW). In the Straits of Sicily area the tEMDW appears as a colder and fresher water mass with respect to the LIW, having a core characterised by a minimum temperature of 13.63°C and a salinity of 38.73.

The intermediate and bottom circulations from historical data as well as from surveys show almost stable situations, mainly shaped by topography. These water masses spread westward as an undercurrent and spill over the sills of the Straits of Sicily, partially compensating the transport of the upper flow and bringing salty and warm waters into the Western Mediterranean.

The horizontal distribution of these multiple water masses gives evidence to the strong mixing processes in action. This system constitutes the basin scale thermohaline core of the Mediterranean circulation that in the Straits of Sicily can be used as indicator of climate change, since each flow is characterised by a significant seasonal and interannual variability. The presence of the different water masses, their paths, and their interactions are the result of local (such as due to upwelling, meandering or eddy phenomena) and large-scale effects.

The seasonal variability of circulation in the central Mediterranean sea has been studied by Sorgente *et al*. (2003)[22] using a high resolution eddy-resolving primitive equation numerical model, based on the Princeton Ocean Model (POM). The model correctly reproduced the seasonal climatological cycle of the circulation in the area, as evidenced by the comparison of the model results with the circulation patterns inferred from the bibliography and from remote sensed thermal Advanced Very High Resolution Radiometer (AVHRR) data. The simulated horizontal fields at 5m and 280m depth, and vertical sections along the meridians 9° E, 13° E and between 11.1° E – 36.85° N and 12.3° E – 38° N (across the Sicily Strait),

[22] Sorgente, R., Drago, A. and Ribotti, A. (2003). Seasonal variability in the Central Mediterranean Sea circulation. *Annales Geophysicae*, 21, 299 - 322.

taken from the fifth year of model integration, are used to describe the phenomenology and the seasonal variability of the 3-D circulation in the model domain. The monthly mean fields of temperature (see section 1.3), salinity (see section 1.4) and velocity (see section 1.5) for February and August are used as the representative months for winter and summer, respectively.

A downscaled description of the seasonal climatological cycle in the area of sea around the Maltese Islands and the Malta Channel is on the other hand provided by Drago *et al.* (2003)[23]. These authors applied a two-step coupling (free-surface/free-surface models nesting on a climatological basis) of the large-scale Mediterranean Ocean General Circulation Model to an embedded primitive equation model with active thermodynamics, implemented over a shelf-scale inner domain (high resolution) covering the Malta Channel and Maltese shelf area (ROSARIO-I), and a regional-scale outer domain (coarse resolution) solution covering the Sicilian Channel area, and subsequently, to a higher resolution shelf-scale implementation with three open boundaries and monthly surface forcing.

Drago *et al.* (2010)[24], used as a numerical model a 3D primitive equation, mesoscale resolving regional ocean model based on POM (Princeton Ocean Model), run over a period of five years (4th January 2000 – 27th December 2004), to show the distribution of the main water masses. Their results are comparable to the literature and confirm the hypothesis of counter phase behaviour for the two main branches of the AC entering in the Straits of Sicily, the ATC stronger in winter and the AIS stronger during summer in the South Central Mediterranean.

1.3 Sea Temperature

Sea temperature varies vertically according to the water masses that make up the water column. Indeed the water masses mentioned in Section 1.2, can all be practically followed by their temperature signatures. Variation is both by season especially when there is water stratification in the summer and water mixing in the winter period and also inter-annually.

Daily high frequency data on average sea temperature is issued by the Physical Oceanographic Unit[25] of the IOI-Malta Operational Centre. The data is recorded in real time by the Malta MedGLOSS station[26] situated at the Portomaso marina in St. Julians, and maintained by the PO-Unit. This station constitutes the first real-time monitoring station for oceanographic data in Malta and forms part of the MedGLOSS sea level network. The instrument, donated by the International Commission for the Scientific Exploration of the Mediterranean Sea (CIESM), collects sea level data (every half-a-minute), seawater

[23] Drago, A.F., Sorgente, R., and Ribotti, A. (2003). A high resolution hydrodynamical 3D model of the Malta Shelf area. In *Annales Geophysicae*, 21: 323-344 pp.

[24] Drago, A., Sorgente, R., and Olita, A. (2010). Sea temperature, salinity and total velocity climatological fields for the south-central Mediterranean Sea. GCP/RER/010/ITA/MSM-TD-14. *MedSudMed Technical Documents*, 14: 35 pp.

[25] The PO-Unit undertakes fundamental research in coastal meteorology, hydrography and physical oceanography with a main emphasis on the experimental study of the hydrodynamics of the sea in the vicinity of the Maltese Islands. More information is available from: http://www.capemalta.net/pounit/

[26] MedGLOSS is a pilot project that is building an operational sea level monitoring network system for systematic measurements in the Mediterranean and Black Seas. The system aims at providing for the first time a high quality standardized data on sea level in near real-time. More information is available from: http://www.capemalta.net/pounit/medgloss.html

temperature, atmospheric pressure and waves in the marina. Data can be viewed online on the website of the PO-Unit[27].

Sea Surface Temperature (at 5m depth) – Characteristics (Seasonal and Annual) and Trends

Sea surface temperature (SST) is relevant for monitoring of climate change because it reflects changes in ocean temperature. Indeed SST in a domain at any time is linked to the persisting surface flows and carries the signature of water masses described in Section 1.2 as they are transformed by different meteorological and mixing conditions. In the area surrounding the Maltese Islands, various phenomena join to produce a very variable and complex SST field. The progression of the AIS and its eastward extension, the upwellings south of Sicily (see Section 1.7) and the warming and cooling of the shallow continental shelf waters are amongst the main driving processes. The annual cycle is indeed rather complex and significant variability can be observed from year to year.

Figure 6: Simulated 10-day averaged temperature field at 5m depth in (a) February & (b) August
Contour interval is 0.5° in February and 1°C in August[28]

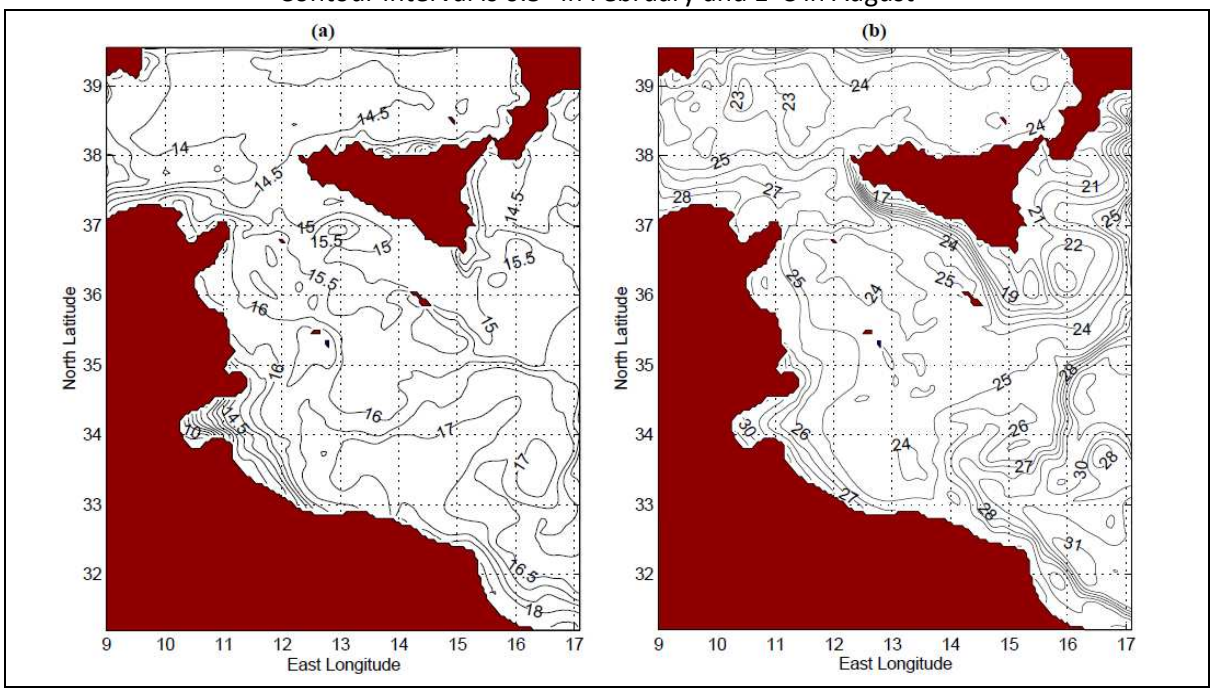

When considering the simulated results of Sorgente *et al*. (2003)[29] for seasonal variability of sea surface temperature (at 5m depth), Figure 6 shows a shift in the mean temperature of about 6°C between February (Figure a representing winter) and August (Figure b representing summer) mainly as a consequence of surface heating. During winter (Figure a), winter mixing processes result in the homogenization of the water column up to depths in excess of 100m, and with temperatures on average 0.5°C higher to the south of Malta. During this time, the thermal structure is fairly homogeneous, especially beyond 35° N

[27] www.capemalta.net

[28] Sorgente, R., Drago, A. and Ribotti, A. (2003). Seasonal variability in the Central Mediterranean Sea circulation. *Annales Geophysicae*, 21, 299 - 322.

[29] Sorgente, R., Drago, A. and Ribotti, A. (2003). Seasonal variability in the Central Mediterranean Sea circulation. *Annales Geophysicae*, 21, 299 - 322.

(including the north side of the Sicily Channel). The temperature does not exceed 15°C. During the summertime, the nearshore well stratified surface layer (averages 20m in depth) above the cooler and relatively fresher Modified Atlantic Water (MAW), due to solar heating, reaches temperatures between 20 and 26°C. In summer (Figure b) the simulated potential temperature is characterised mainly by upwelling events along the southern coast of Sicily, bringing cooler water to the surface (see also section 1.7 of this Chapter). This is in contrast to the overall increase in temperature over the region. Warm waters have a mean temperature of over 26°C. The contrast in temperature of the MAW exiting the Sicilian Channel with the warmer Ionian water produces a sharp temperature gradient (Figure b) which is often evidenced over the Malta escarpment by conspicuous thermal features on the sea surface temperature AVHRR.

The following figures also depict SST in correlation to the characteristics and trends of oceanographic processes pertaining to the area on the basis of the works of Drago*et al.* (2003)[30] and Alpha Briggs (2008) [31].

[30] Sorgente, R., Drago, A. and Ribotti, A. (2003). Seasonal variability in the Central Mediterranean Sea circulation. *Annales Geophysicae*, 21, 299 - 322.

[31] Alpha Briggs (2008). Hydrographic Data Report. 102pp.

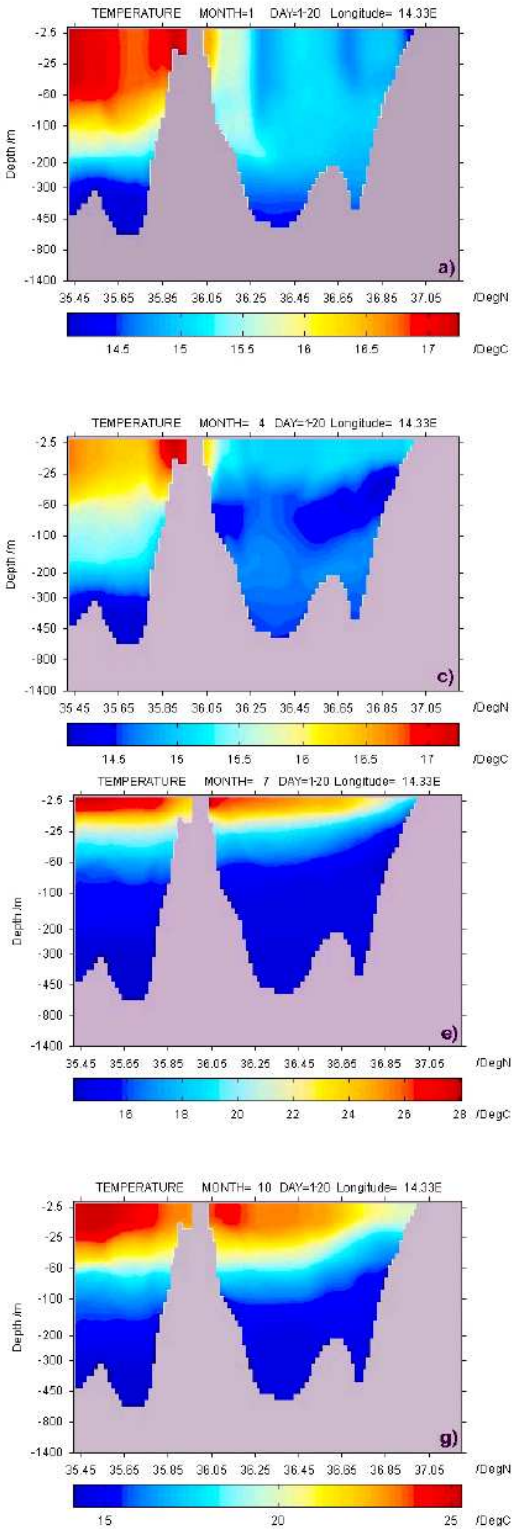

Figure 7: Meridional sections of temperature along latitude 14°20′ E, plotted from 10-day averaged fields in (second third of) January, April, July and October [Source: Drago, Sorgente and Ribotti (2003)]

Figure 7 to the left depicts meridional sections of temperature for months 1 (winter), 4 (spring), 7 (summer) and 10 (autumn). The plotting of temperature at 5m depth provides better compatibility with satellite-derived sea surface temperature images. The vertical section is taken along longitude 14°20′ E to coincide with the dividing line between Malta and Gozo, cutting across the Gela Sicilian basin, and meeting that part of the Sicilian coast which appears from satellite data to be a focal starting location for upwelling events. In consequence of the sustained surface evaporation caused by the increase in solar heating, the upper MAW layer in summer (see Figure for month 7) is characterised by a high temperature ranging from 20°C to 27°C from north to south. Approaching the winter season strong surface cooling and vertical mixing come into action (see Figure for month 1). A single homogeneous water mass is formed in the Malta Channel up to a depth of 100m with temperatures around 15°C; to the south the upper layer temperatures are around 2°C higher (homogeneous up to 60 m) mainly due to the advection of warmer water from the south. The Maltese Islands are thus, very often situated within a frontal zone, with appreciable differences in temperature between the northern and southern shores. In early spring (see Figure for month 4) the presence of the fresh MAW starts to regain its evidence between Malta and Sicily, but its temperature in the upper layer remains greatly conditioned by surface forcing.

Figure 8 also shows the complexity of the annual cycle that is representative of the average background synoptic situation. It is mainly characterised by cooler and commonly homogeneous waters in the Malta Channel, especially in winter and early spring, while much warmer waters lie to the south of the Maltese Islands. This contrast often results in a broad and long front produced from the contrast at the northern border of the warm Sidra gyre (to the south of Malta) with the southern extremity of the colder vein of MAW along the AIS. This front can occasionally be shifted to lie in very close proximity to Malta. The Maltese Islands are thus very often situated within the frontal line so that temperature differences between the northern and southern shores become appreciable in such circumstances. The end of May usually leads to the first summer features. The reduced surface cooling and the presence of stratification mark the onset of upwelling zones and fronts.

Figure 8: Seasonal Sea Surface Temperature maps[32]

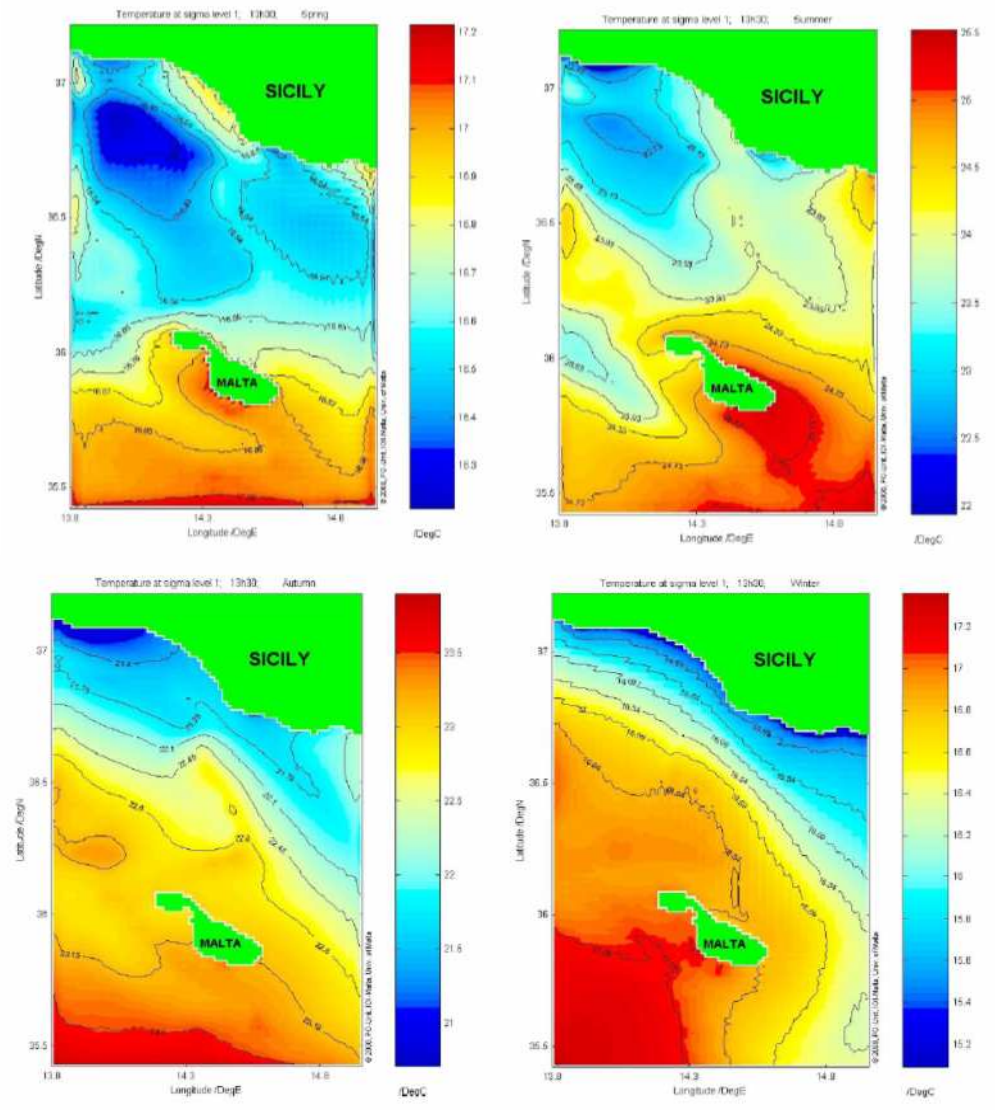

[32] Source: Alpha Briggs (2008). Hydrographic Data Report. 102pp.

The marked zone of cooler water to the west of Gozo in summer is related to the anticyclonic (clockwise) circulation present in this area; geotropic forces associated with this mesoscale gyre give rise to a radial transport of water away from its centre and an associated vertical pumping of subsurface cooler water that rises to the surface at its centre. The generally warmer waters on the south-eastern coastal areas of Malta are similarly associated to the clockwise circulation around the tip of the island, which tend to trap water against the coast and tend to maintain slightly higher temperatures.

Figure 9: Annual Sea Surface Temperature map[33]

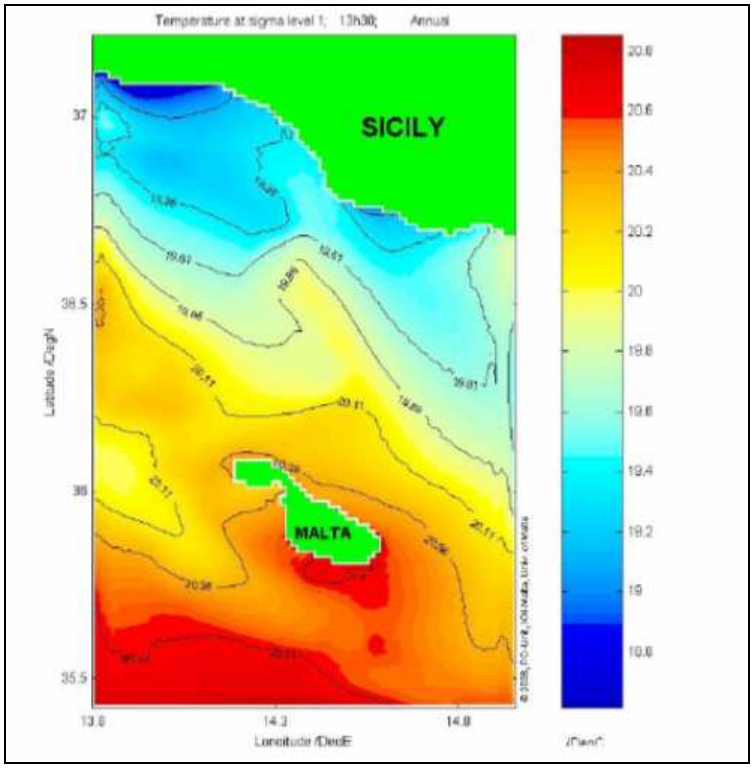

The progression of the AIS and its south-eastward extension is delineated by the 19.86°C isotherm in the annual mean map (Figure 9).

Similar seasonal changes in sea surface temperature at a depth of 5m during the year 2010 are also shown at sub-basin level in Figure 10, while Figure 11 shows annual variation between the period 2008 to 2010.

[33] Source: Alpha Briggs (2008). Hydrographic Data Report. 102pp.

Figure 10: Sea Surface Temperature at 5m depth (Monthly for 2010); Sicily Strait sub-Regional Model (SCRM)[34]

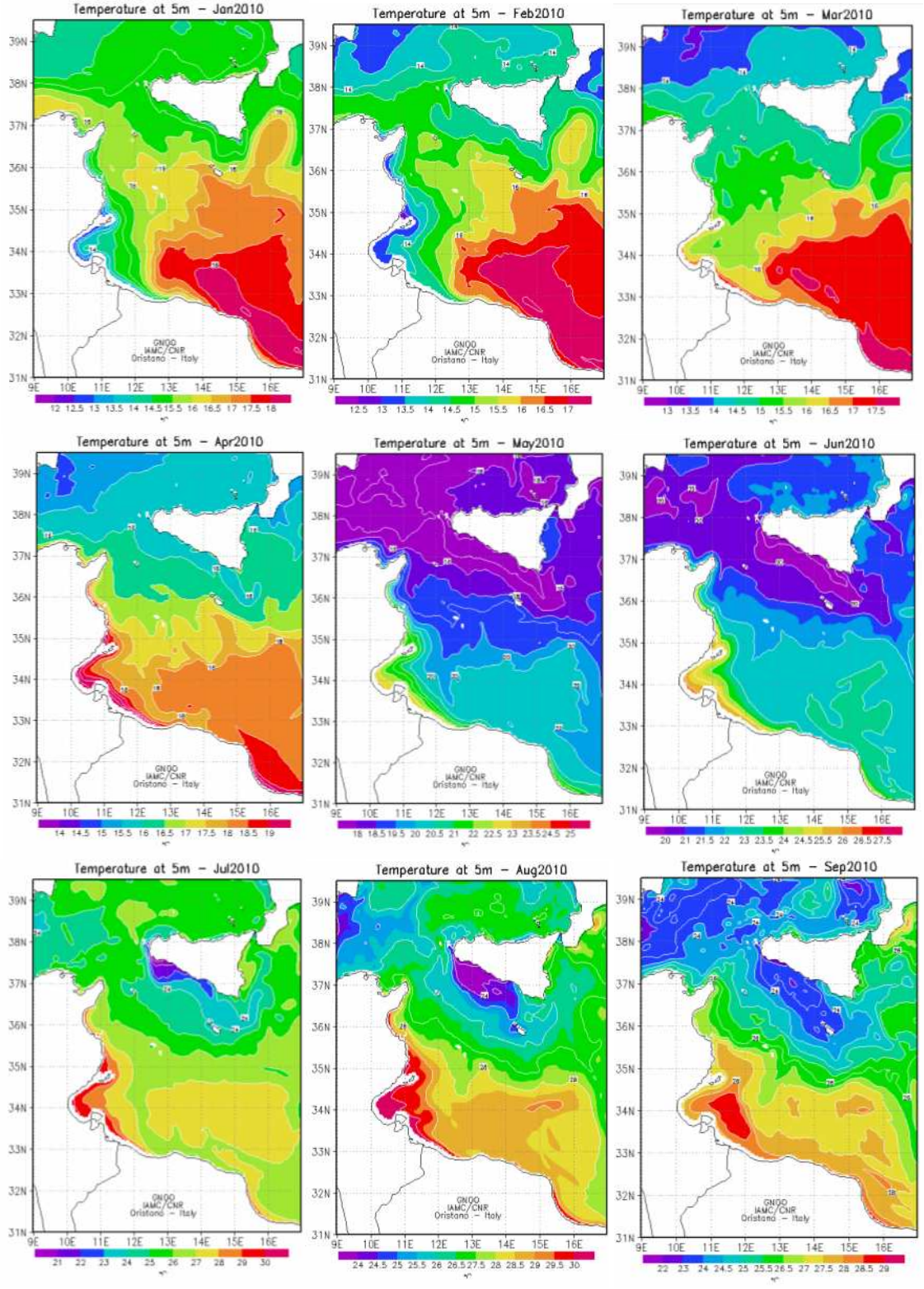

[34] Source: G30 – IAMC – CNR of Oristano http://www.seaforecast.cnr.it/en/fl/climatology.php

Figure 10 continued: Sea Surface Temperature at 5m depth (Monthly for 2010); Sicily Strait sub-Regional Model (SCRM)[35]

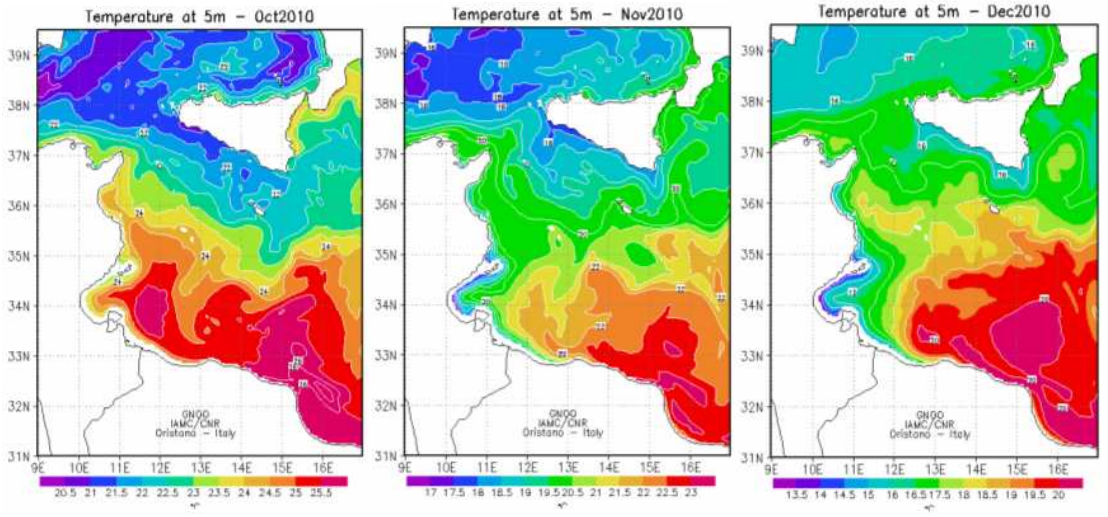

Figure 11: Sea Surface Temperature at 5m depth (Yearly - 2008 to 2010); Sicily Strait sub-Regional Model (SCRM)[36]

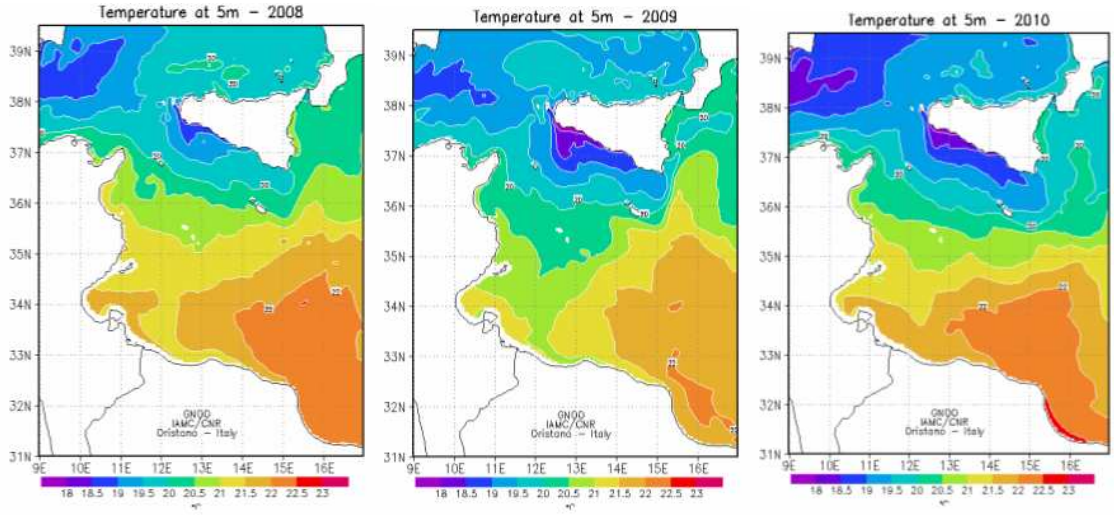

[35] Source: G30 – IAMC – CNR of Oristano http://www.seaforecast.cnr.it/en/fl/climatology.php

[36] Source: G30 – IAMC – CNR of Oristano www.seaforecast.cnr.it/en/fl/yearly.php

Sea surface temperature is also one of the physicochemical parameters that are monitored in compliance with the Water Framework Directive. The method employed is APAT CNR IRSA 2100 Man 29 2003. Sea surface temperature readings are shown in Table 1 for the year 2012 between the months of May and November. As seen in the graph (Figure 12 - shows only sites which have a complete set of readings), the sea surface temperature increases on approaching summertime with readings peaking in the survey carried out at the end of August/ beginning of September, which reflects the surface heating (max reading is 29.15°C) that is normal for that time of year, following which the temperature starts to decrease on approaching the months of October and November.

Table 1: Sea Temperature Readings at 5m depth obtained using a multi-parametric probe (Mean & SDs)[37]

2012						
Monitoring Position	**1st Survey End May/ Beginning June**	**2nd Survey End June/ Beginning July**	**3rd Survey Beginning of August**	**4th Survey End Aug/ Beginning Sep**	**5th Survey End Sep/ Beginning Oct**	**6th Survey End Oct/ Beginning Nov**
CN01-1		26.08± 0.1 2 July	25.3± 0.14 1 Aug	27.15± 0.07 29 Aug	25.32±0.31 5 Oct	24.63±0.176 26 Oct
CN01-2	19.96± 0.03 30 May	25.58± 0.1 2 July	25.8± 0.0 1 Aug	27.4± 0.00 29 Aug	25.61±0.06 5 Oct	24.31±0.00 26 Oct
CN02-1		26.65± 0.07 2 July	24.9± 0.14 1 Aug	27.85± 0.07 29 Aug	24.75±0.94 5 Oct	24.27±0.049 26 Oct
CN03-1	20.01± 0.06 30 May		27.1± 0.14 2 Aug	27.75± 0.07 29 Aug	25.26±0.08 28 Sep	24.53±0.00 26 Oct
CN03-2		25.86± 0.04 2 July	27.4± 0.28 2 Aug	27.7± 0.00 29 Aug	24.2±0.028 28 Sep	24.41±0.134 26 Oct
CN04-1	20.07± 0.08 31 May	25.25± 0.08 27 June	27.7± 0.28 3 Aug	28.1± 0.14 29 Aug	25.255±0.22 28 Sep	24.33±0.127 26 Oct
CN04-2		25.64± 0.08 27 June	27.9± 0.14 7 Aug	28.05± 0.07 30 Aug	25.61±0.06 6 Oct	24.5±0.523 26 Oct
CN04-4		26.01± 0.13 27 June	27.9± 0.28 3 Aug	27.75± 0.07 30 Aug	26.06±0.07 6 Oct	24.16±0.084 26 Oct
CN04-5		25.77± 0.06 27 June	27.5± 0.42 6 Aug	28.05± 0.07 30 Aug	25.72±0.06 6 Oct	24.22±0.127 26 Oct
CN04-6		25.88± 0.17 27 June	26.8± 0.0 6 Aug	28.1± 0 30 Aug	25.89±0.13 6 Oct	24.285±0.388 26 Oct
CN05-1	21.13± 0.07 4 June	26.63± 1.53 27 June	26.9± 0.14 6 Aug	28.55± 0.07 30 Aug	25.85±0.00 6 Oct	24.37±0.042 26 Oct
CN06-1		26.58± 0.03 3 July	26.9± 0.28 6 Aug	28.55± 0.07 30 Aug	25.37±0.04 6 Oct	24.35±0.070 4 Nov
CN07-1	20.04± 0.07 2 June	26.22± 0.13 3 July	27.8± 0.42 6 Aug	28.4± 0.00 30 Aug	25.48±0.17 6 Oct	24.495±0.063 4 Nov
CN07-2		25.36± 0.08 3 July	27.1± 0.14 5 Aug	28.25± 0.07 30 Aug	24.49±0.30 6 Oct	24.4±0.141 4 Nov
CN07-3		25.55± 0.03 3 July	25.7± 0.28 5 Aug	28.4± 0.00 30 Aug	25.16±0.23 6 Oct	24.7±0.141 4 Nov
CN09-1		25.89± 0.01 2 July	26.4± 0.14 2 Aug	27.75± 0.07 29 Aug	24.8±0.00 28 Sep	24.87±0.00 26 Oct
CP04-1	20.18± 0.07 31 May	25.55± 0.06 27 June	27.3± 0.14 6 Aug	28± 0.00 30 Aug	25.50±0.07 6 Oct	24.36±0.197 26 Oct
CP04-2		25.59± 0.07 27 June	27.8± 0.14 7 Aug	27.75± 0.07 30 Aug	25.50±0.07 6 Oct	24.355±0.06 26 Oct
CP05		26.88± 0.11 3 July	27.4± 0.42 6 Aug	29.15± 0.07 30 Aug	26.27±0.05 6 Oct	24.46±0.33 26 Oct
CP06-1	20.62± 0.04 4 June	26.51± 0.06 3 July	27.4± 0.28 6 Aug	28.1± 0.14 30 Aug	25.55±0.13 6 Oct	24.15±0.212 4 Nov
CP07	19.95± 0.04 2 June	25.99± 0.07 3 July	27.8± 0.14 5 Aug	28.5± 0.00 30 Aug	24.54±0.37 6 Oct	24.22±0.00 4 Nov
CS01		26.72± 0.04 2 July	25.4± 0.0 1 Aug	27.2± 0.00 29 Aug	25.29±0.37 5 Oct	24.56±0.00 26 Oct
CS02	20.02± 0.03 30 May	26.55± 0.1 2 July	25.6± 0.28 1 Aug	27.8± 0.00 29 Aug	24.72±0.84 5 Oct	24.36±0.056 26 Oct
CS03	19.85± 0.06 6 June	26.33± 0.06 2 July	26.9± 0.14 3 Aug	27.55± 0.07 29 Aug	24.325±0.18 28 Sep	24.33±0.127 26 Oct
CS08		26.01± 0.64 3 July	27.1± 0.28 5 Aug	28.45± 0.07 30 Aug	24.70±0.00 6 Oct	24.395±0.077 4 Nov
CS09	21.63± 0.1 2 June	25.84± 0.04 2 July	26.6± 0.0 2 Aug	28.1± 0.14 29 Aug	25.3±0.00 28 Sep	24.73±0.00 26 Oct

[37] CIBM and Ambiente SC (2013) Development of Environmental Monitoring Strategy and Environmental Monitoring Baseline Surveys – Water Lot 3 – Surveys of Coastal Water – August 2012. ERDF156 - Developing national environmental monitoring infrastructure and capacity

Figure 12: Sea Surface Temperature (°C) between May and November for the Year 2012

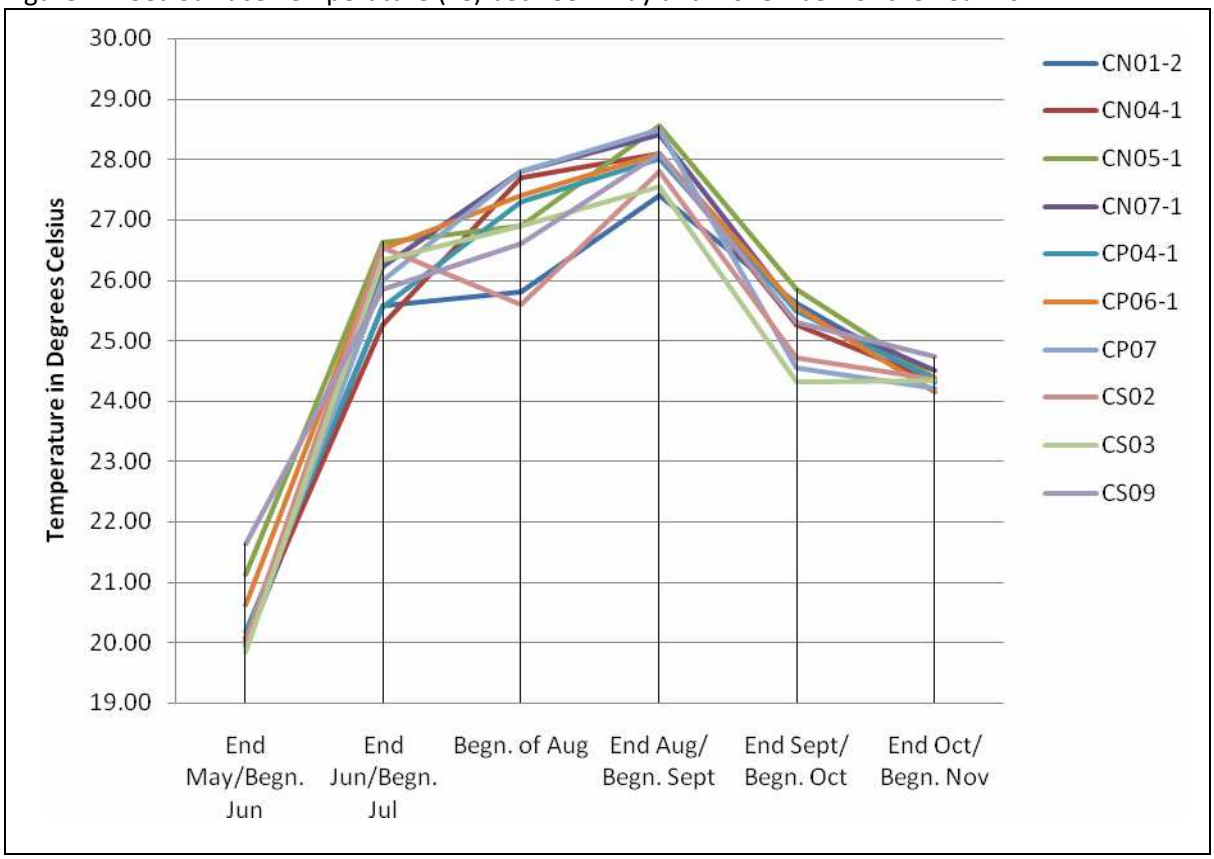

Sea surface temperature is also monitored in coastal bathing waters as part of the bathing quality monitoring programme. The parameter is recorded using an Eil Type M.C.5 Induction meter. SST monitoring in June 2003 and March 2004 (Axiaq 2004)[38] produced readings that express typical seasonal fluctuations for local coastal waters. Exceptions in the form of high temperature anomalies are recorded at sites exposed to thermal discharges of cooling waters from power stations at Marsa (Marsa PS) and Hofra iż-Żgħira (Delimara PS). In these areas temperatures of surface and sub-surface waters at distances varying from 25 to 50m away from the discharge points increased by 5.4 to 5.5°C above ambient.

[38] Axiaq, V. (2004) Marine Coastal Monitoring Programme: June 2003, March 2004

When considering trends, the IPCC Fourth Assessment Report on Climate Change (2007) mentions the "[while there are strong natural variations in the Mediterranean, overall there is a discernible trend of increased salinity and warmer temperature in key water masses over the last 50 years". Trends in increasing sea surface temperature in European Seas including Mediterranean Sea are also reported by the EEA (2010)[39]. The EEA's 2010 report on the State and Outlook of the Marine and Coastal mentions that changes in SST have been up to six times greater in European Seas than in the global oceans in the past 25 years. The most rapid warming trend is in the Baltic and North Seas, while the rates are lower in the Black and Mediterranean Seas. Such changes have not been observed in any other 25-year period since systematic observations started more than a century ago (Figure 13).

On a local scale, Malta's Second National Communication to the United Nations Framework Convention on Climate Change (UNFCCC)[40] states that the mean SST in the coastal waters of the Maltese Islands has been steadily increasing at an average rate of close to +0.05°C per year since the late 70s. This is based on measurements made at a constant single point (in the open sea outside Delimara point) and at the same level of about 1 m below the sea surface, conducted for 28 consecutive years. The increase in SST in Malta is most evident during summer, although it is also high in autumn and to some extent in winter, which is clear evidence that the sea temperature depends also on non-local larger scale phenomena.

Figure 13: Time series of annual average sea surface temperature (°C), referenced to the average temperature between 1986 and 2010, in each of the European seas[41].

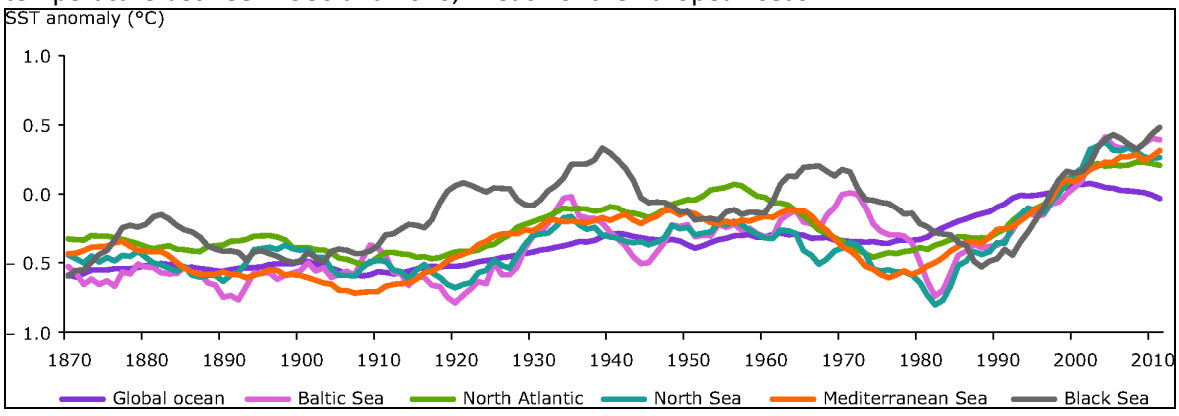

[39] EEA (2010). *The European Environment: State and Outlook 2010 – Marine and Coastal Environment*. Luxembourg: Publications Office of the European Union, 2010.

[40] Ministry for Resources and Rural Affairs & University of Malta 2010 The Second Communication of Malta to the United Nations Framework Convention on Climate Change; http://unfccc.int/resource/docs/natc/mlt_nc02.pdf

[41] Data sources: SST datasets from the Hadley Centre (HADISST1 (global)), MOON-ENEA (Mediterranean Sea), and Bundesamt für Seeschifffahrt und Hydrographie (Baltic and North Seas), and MyOcean. Web Source: http://www.eea.europa.eu/data-and-maps/figures/annual-average-sea-surface-temperature

Near-Bottom Temperature (at 280m depth) – Characteristics (Annual & Seasonal) and Trends

When considering the work of Drago *et al*. (2003)[42], and referring back to Figure 7, in the summer period (see Figure for month 7), the near-bottom temperature is between 16°C and 19°C. Approaching the winter season strong surface cooling and vertical mixing come into action (see Figure for month 1). A single homogeneous water mass is formed in the Malta Channel up to a depth of 100m with temperatures around 15°C; to the south the upper layer temperatures are around 2°C higher (homogeneous up to 60 m) mainly due to the advection of warmer water from the south. A transition stable water layer resides between around 100m and 200m depth with an average temperature of 15.5°C (see Figures for all months). The characteristics of this layer are rather persistent throughout the year except that it is less thick in winter (see Figure for month 1). In agreement with the MEDATLAS I data set the deeper water mass resides below 250m in winter and has a temperature decreasing with depth from 14.7°C to 14°C. This water mass is identified as the MLIW and is practically absent over the Malta shelf areas with depths shallower than 100 m.

A predominant, well-defined north westerly flux of saline MLIW flowing over the slope to the south of Malta exists in winter, with its main core centred at around 280m and with a vertical extent of more than 200m. It is characterised by a very stable temperature of around 14.8°C. It attenuates somewhat in spring, moving to a slightly deeper position in summer when it becomes even weaker.

1.4 Sea Salinity – Characteristics and Trends

The Mediterranean Sea characteristically has a high salinity due to high evaporation rates and low river run-off. The simulated 10-day averaged salinity field at 5m depth (Figure 14) shows the seasonal signature of the MAW flow as an extension of the Algerian coastal current into the Sicilian Channel and beyond as an unstable flux of relative fresh water. It is identified by a salinity in the range from 37.2 to 37.7 psu, and its horizontal variation shows the gradual modification of its properties as it penetrates from west to east across the domain. During the summertime, sustained sea surface evaporation rates increase the salinity, which reaches maximum values of S = 38.0 to the south of Malta.

[42] Drago, A.F., Sorgente, R., and Ribotti, A. (2003). A high resolution hydrodynamical 3D model of the Malta Shelf area. In *Annales Geophysicae*, 21: 323-344 pp.

Figure 14: Simulated 10-day averaged salinity field at 5m depth in (a) February and (b) August; Contour interval is 0.1 psu[43]

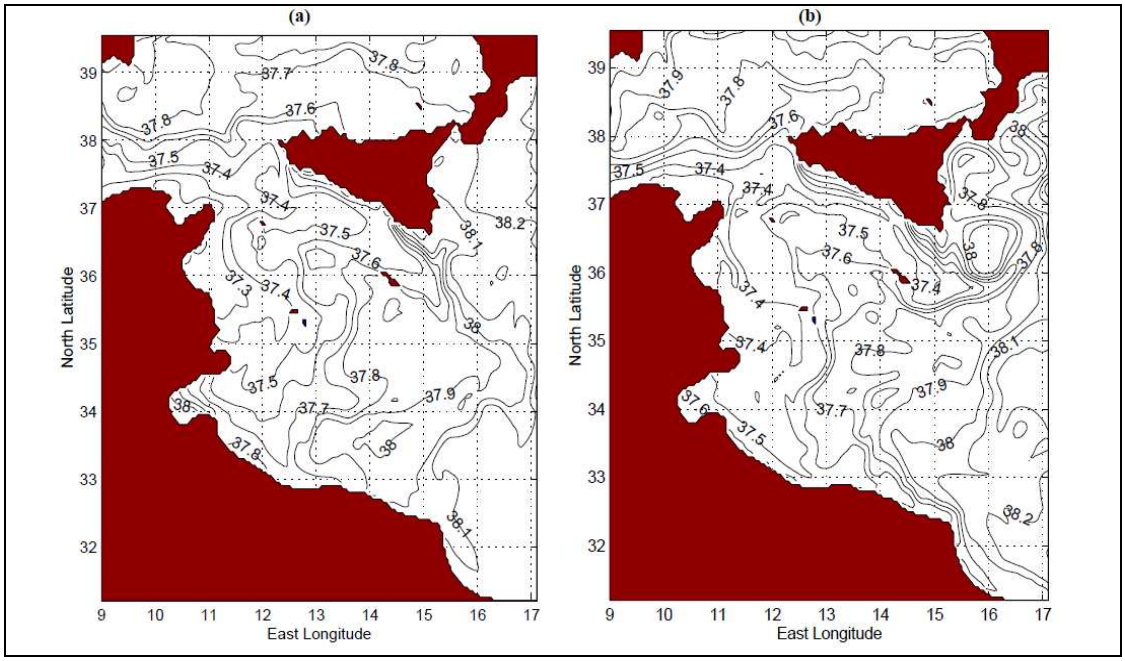

[43] Sorgente, R., Drago, A. and Ribotti, A. (2003). Seasonal variability in the Central Mediterranean Sea circulation. *Annales Geophysicae*, 21, 299 - 322.

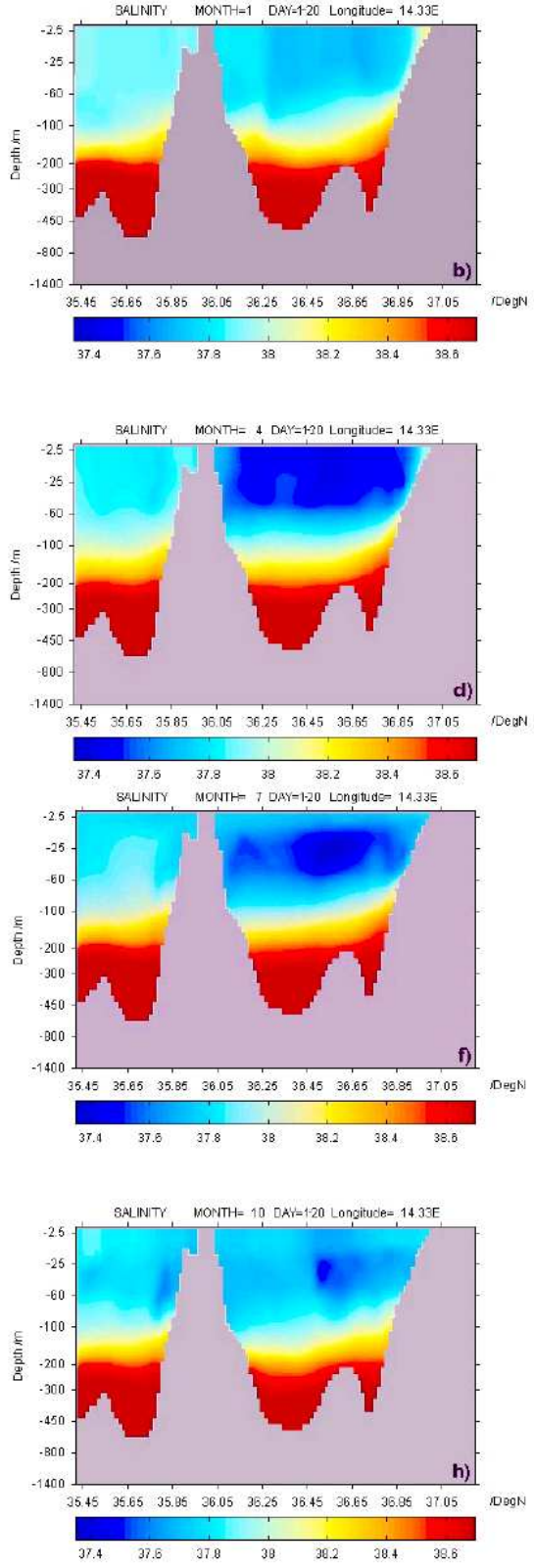

Figure 15: Meridional sections of salinity along latitude 14°20′ E, plotted from 10-day averaged fields in (second third of) January, April, July and October [Source: Drago, Sorgente and Ribotti (2003)]

Figure 15 to the left, depicts meridional sections of salinity in months 1 (winter), 4 (spring), 7 (summer) and 10 (autumn) on the basis of the work by Drago *et al*. (2003)[44]. The model simulations clearly show the strong seasonal variability in the salinity of the surface MAW, as well as in the thickness of this layer. The upper water layer in summer is characterised by a maximum salinity (reaching an average of 37.8 psu to the south). The underlying water has a lower salinity of the order of 37.4 psu, thus presenting, especially in the north, a salinity minimum with respect to the surface water. In mid-July this water of Atlantic origin appears as a well-defined subsurface core, centred along 36.6° N of latitude at an average depth of 20 to 60m (see Figure for month 7). This agrees with the general situation in the broader Sicily Channel area, where the signature of the MAW is represented by a salinity minimum situated at about 50m in depth during summer and near the surface during winter. This core is gradually eroded as the winter season is approached, and strong surface cooling and vertical mixing come into action. A single homogeneous water mass is formed in the Malta Channel up to a depth of 100m (see Figure for month 1). In early spring the presence of the fresh MAW starts to regain its evidence between Malta and Sicily. A transition stable water layer resides between around 100m and 200m depth with an average salinity of 38.2 psu. This intermediate water is more saline than the overlying water masses and is the result of mixing of the Atlantic water with the deeper more dense water. The characteristics of this layer are rather persistent throughout the year (see Figures for all months) except that it is less thick in winter (see Figure for month 1). In agreement with the MEDATLAS I data

[44] Drago, A.F., Sorgente, R., and Ribotti, A. (2003). A high resolution hydrodynamical 3D model of the Malta Shelf area. In *Annales Geophysicae*, 21: 323-344 pp.

set the deeper water mass resides below 250m in winter and has a uniform salinity of around 38.75 psu (see Figures for all months). This water mass is identified as the MLIW and is practically absent over the Malta shelf areas with depths shallower than 100 m. It presents a maximum salinity in the western and southwestern approaches of Malta. The renewal time of the total MLIW in the channel has been estimated to be around 9 months, which is long enough to explain the fairly constant salinity over the annual cycle.

Annual changes in salinity at a depth of 5m between the period 2008 to 2010 are shown at sub-basin level in Figure 15.

Figure 15: Sea Salinity at 5m depth (Annual from 2008 to 2010) Sicily Strait sub-Regional Model (SCRM)[45]

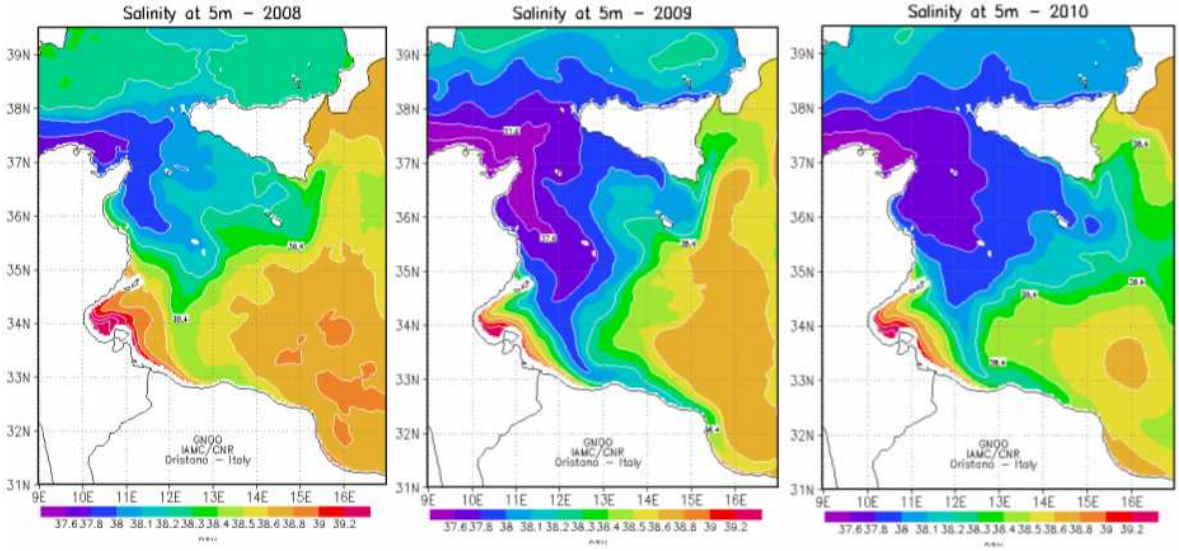

Sea salinity is monitored in coastal bathing waters as part of the bathing quality monitoring programme. The parameter is recorded using an Eil Type M.C.5 Induction meter. Salinity of inshore waters ranged from 36.7 to 39.2 for June 2003 and from 35.1 to 38.9 for March 2004. In some cases, especially in inshore semi-enclosed creeks, surface salinities could fluctuate over a higher range, due to being influenced to a greater extent by land runoff water. Localised regions of very low salinity were usually those exposed to point source land-based discharges such as sewage outfalls (Axiaq, 2004)[46]. It should be noted that all untreated sewage outfalls have (since 2011) been replaced by treated sewage effluents.

Sea salinity is also one of the physicochemical parameters that is monitored in compliance with the Water Framework Directive. The method employed is APAT CNR IRSA 2070 Man 29 2003. Salinity readings (‰) are shown in

[45] Source: G30 – IAMC – CNR of Oristano - http://www.seaforecast.cnr.it/en/fl/yearly.php
[46] Axiaq, V. (2004) Marine Coastal Monitoring Programme: June 2003, March 2004

Table 2 and Figure 16.

Table 2: **Salinity readings at a depth of 5m using a multi-parametric probe (means and SD)**[47]

2012						
Monitoring Position	**1st Survey 29 May to 6 June**	**2nd Survey 27 June and 2-3 July**	**3rd Survey Beginning of August**	**4th Survey End Aug/ Beginning Sep**	**5th Survey End Sep/ Beginning Oct**	**6th Survey End Oct/ Beginning Nov**
CN01-1		33.35± 0.03 2 July	37.6± 0.14 1 Aug	40.61± 0.01 29 Aug	38.60±0.00 5 Oct	37.385±0.318 26 Oct
CN01-2	38.64± 0.04 30 May	30.58± 0.03 2 July	38.6± 0.0 1 Aug	40.63± 0.03 29 Aug	38.61±0.01 5 Oct	38.34±0.12 26 Oct
CN02-1		28.96± 0.07 2 July	37.4± 0.14 1 Aug	40.61± 0.01 29 Aug	38.61±0.01 5 Oct	38.77±0.254 26 Oct
CN03-1	38.67± 0.01 30 May		37.8± 0.42 2 Aug	41.02± 0.02 29 Aug	38.1±0.14 28 Sep	38.445±0.205 26 Oct
CN03-2		30.73± 0.04 2 July	35.6± 0.28 2 Aug	39.83± 0.04 29 Aug	38.9±0.00 28 Sep	38.495±0.063 26 Oct
CN04-1	38.65± 0 31 May	30.18± 0.1 27 June	37.5± 0.0 3 Aug	38.95± 0.66 29 Aug	38.41±0.01 28 Sep	38.535±0.233 26 Oct
CN04-2		30.29± 0.11 27 June	37.4± 0.28 7 Aug	39.25± 0.69 30 Aug	38.60±0.00 6 Oct	36.345±0.219 26 Oct
CN04-4		32.24± 0.04 27 June	37.9± 0.28 3 Aug	39.53± 0.04 30 Aug	38.74±0.08 6 Oct	37.74±0.33 26 Oct
CN04-5		30.12± 0.03 27 June	36.4± 0 6 Aug	39.65± 0.13 30 Aug	38.57±0.00 6 Oct	36.4±0.042 26 Oct
CN04-6		33.07± 0.11 27 June	37.1± 0.28 6 Aug	39.28± 0.04 30 Aug	38.58±0.01 6 Oct	37.4±0.070 26 Oct
CN05-1	38.6± 0.04 4 June	30.16± 0.07 27 June	38.9± 0.14 6 Aug	39.47± 0.35 30 Aug	38.31±0.29 6 Oct	37.595±0.077 26 Oct
CN06-1		32.65± 0.01 3 July	37.6± 0.28 6 Aug	39.47± 0.38 30 Aug	38.51±0.01 6 Oct	38.2±0.282 4 Nov
CN07-1	38.68± 0.04 2 June	29.99± 0.06 3 July	38.9± 0 6 Aug	39.76± 0.49 30 Aug	38.36±0.17 6 Oct	35.3±0.141 4 Nov
CN07-2		32.66± 0.03 3 July	37.5± 0.14 5 Aug	39.98± 0.24 30 Aug	38.44±0.25 6 Oct	38.05±0.212 4 Nov
CN07-3		25.7± 0.08 3 July	38.9± 0.14 5 Aug	38.83± 1.51 30 Aug	38.27±0.05 6 Oct	38.385±0.318 4 Nov
CN09-1		29.92± 0.1 2 July	38.5± 0 2 Aug	39.11± 0.01 29 Aug	38.61±0.00 28 Sep	38.63±0.00 26 Oct
CP04-1	38.65± 0 31 May	30.24± 0.07 27 June	35.9± 0.14 6 Aug	39.24± 0.02 30 Aug	38.44±0.25 6 Oct	36.76±0.00 26 Oct
CP04-2		29.97± 0.07 27 June	38.64± 0.04 7 Aug	39.31± 0.01 30 Aug	38.27±0.05 6 Oct	38.335±0.120 26 Oct
CP05		32.68± 4.14 3 July	38.8± 0.28 6 Aug	39.18± 0.59 30 Aug	38.61±0.01 6 Oct	36.76±0.00 26 Oct
CP06-1	38.59± 0.03 4 June	28.97± 0.06 3 July	38.4± 0.14 6 Aug	39.57± 0.16 30 Aug	38.51±0.01 6 Oct	38±0.282 4 Nov
CP07	34.86± 0.06 2 June	32.67± 0.08 3 July	37.8± 0.0 5 Aug	39.55± 0.35 30 Aug	38.31±0.29 6 Oct	37.32±0.113 4 Nov
CS01		33.15± 0.06 2 July	38.4± 0.28 1 Aug	40.56± 0.01 29 Aug	38.60±0.01 5 Oct	38.605±0.09 26 Oct
CS02	38.57± 0.04 30 May	29.51± 0.04 2 July	38.4± 0.0 1 Aug	39.85± 0.02 29 Aug	38.61±0.01 5 Oct	38.15±0.35 26 Oct
CS03	38.57± 0.04 6 June	28.64± 0.03 2 July	38.4± 0.14 3 Aug	39.51± 0.01 29 Aug	38.41±0.30 28 Sep	38.35±0.35 26 Oct
CS08		28.69± 0.04 3 July	38.5± 0.42 5 Aug	39.85± 0 30 Aug	37.10±0.00 6 Oct	37.95±0.070 4 Nov
CS09	38.49± 0.01 2 June	31.02± 0.06 2 July	38.4± 0.14 2 Aug	39.78± 0.04 29 Aug	37.32±0.11 28 Sep	36.86±0.16 26 Oct

[47] CIBM and Ambiente SC (2013) Development of Environmental Monitoring Strategy and Environmental Monitoring Baseline Surveys – Water Lot 3 – Surveys of Coastal Water – August 2012. ERDF156 - Developing national environmental monitoring infrastructure and capacity

Figure 16: Salinity (‰) between May and November for the Year 2012

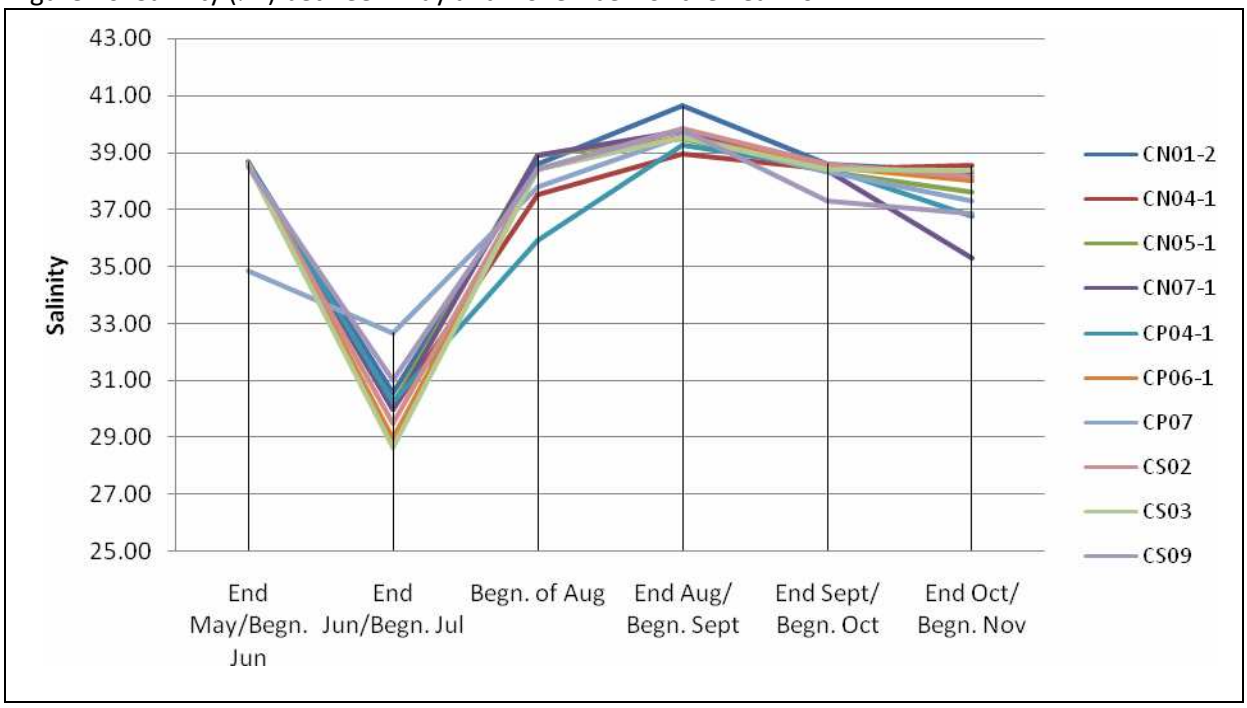

1.5 Sea Current Velocity

The climatology maps in Figure 17 and Figure 18 confirm that the sea surface currents on the Malta shelf area are mainly characterised by the swift AIS directed towards the south-south-east along the Malta Channel and with an average magnitude of 30 cm s^{-1}. The AIS is stronger in summer/autumn and weaker in winter/spring. In the eastern proximities of Malta, the AIS generally tends to swerve towards south; this swerving is most evident in spring, summer and autumn giving rise to strong flows towards the south that subsequently veer towards the south-west. To the west, a quasi-permanent anticyclonic gyre is present; it tends to drive water to the south and south-westerly directions. This circulation is most evident in spring and summer. Annual and seasonal average currents to the south-west of the Maltese Islands are relatively much weaker (10 cm s^{-1} on average) and carry a homogeneous directional spectrum (only a slightly higher frequency of occurrence towards the south-western sector).

Figure 17: Seasonal sea currents climatological maps[48]

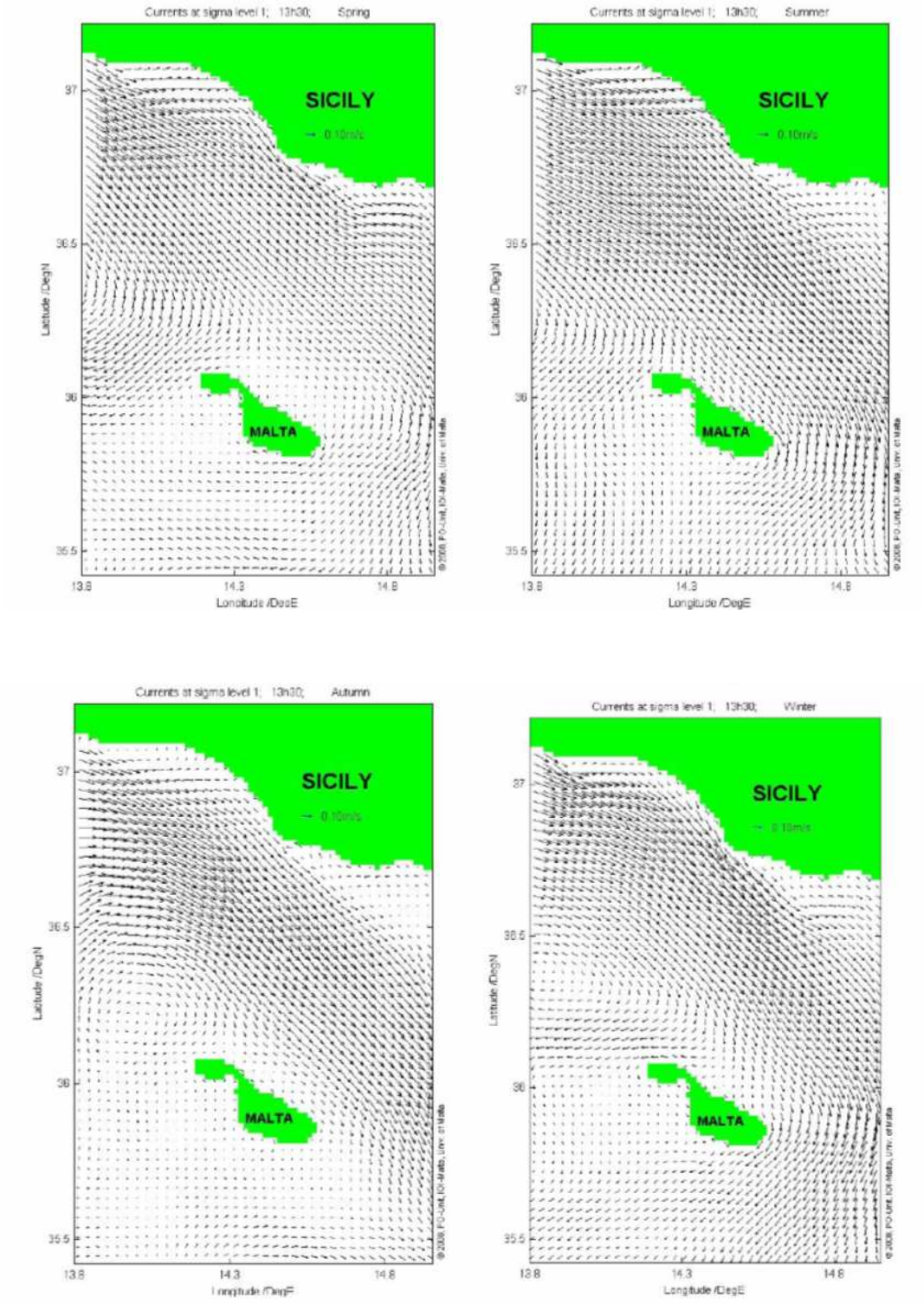

[48] Source: Alpha Briggs (2008). Hydrographic Data Report. 102pp.

Figure 18: Annual sea surface currents climatological map[49]

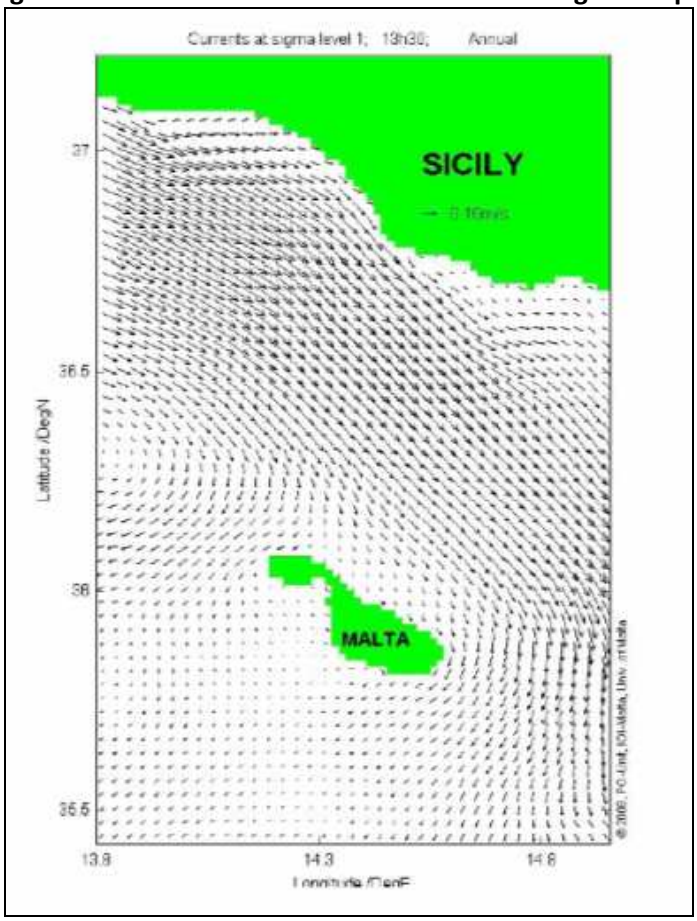

For both the MAW and LIW, the averaged kinetic variability has been observed two to four times higher in winter than in summer, in response to stronger wind stress and reduced stratification. The hydrographic properties of the MAW are also known to undergo significant seasonal variations, but those of the LIW are more constant (see Lermusiaux and Robinson, 2001).

The simulated 10-day averaged total velocity field at 5m depth (Figure 19) shows the seasonal signature of the MAW flow, which can be followed as an extension of the Algerian coastal current into the Sicilian Channel and beyond as an unstable flux of relative fresh water.

[49] Source: Alpha Briggs (2008). Hydrographic Data Report. 102pp.

Figure 19: Simulated 10-day averaged total velocity field at 5m depth in (a) February (Winter) and (b) August (Summer)[50]; One vector every four grid points is plotted. Units are m/s

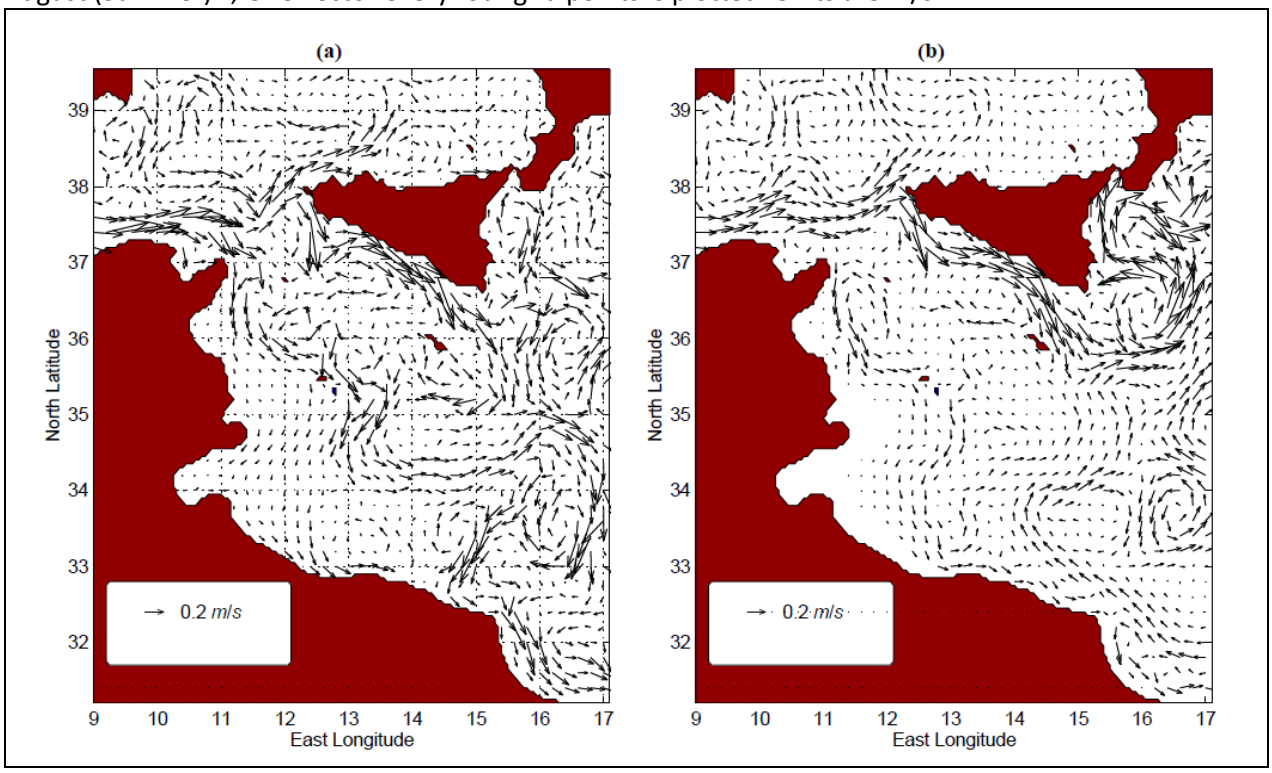

The model results obtained by Sorgente *et al*. (2003)[51] also show the presence of mesoscale extensions and dynamic patterns associated with the instability of the AIS. The flow has a quasi-barotropic nature in the top layer, but is accompanied by strong velocity shears in the bottom boundary layer and along its lateral boundaries as it extends horizontally down to a latitude of 36.4° N, and vertically beyond the Sicilian shelf break. During winter, the AIS is less intense and the MAW flow tends to be more spread along the interior of the Sicilian Channel. There is a decrease in the amplitude of the intense looping meander in the upper Ionian Sea, and the exit of the MAW is shifted further south where the shelf break slope is more tenuous, with the consequence that the fate of the MAW is more probable to branch southward and south eastward, feeding the mid- Mediterranean jet.

[50] Sorgente, R., Drago, A. and Ribotti, A. (2003). Seasonal variability in the Central Mediterranean Sea circulation. *Annales Geophysicae*, 21, 299 - 322.

[51] Sorgente, R., Drago, A. and Ribotti, A. (2003). Seasonal variability in the Central Mediterranean Sea circulation. *Annales Geophysicae*, 21, 299 - 322.

Figure 20: Simulated 10-day averaged total velocity field at 280m depth in (a) February & (b) August[52]; One vector every four grid points is plotted. Units are m/s

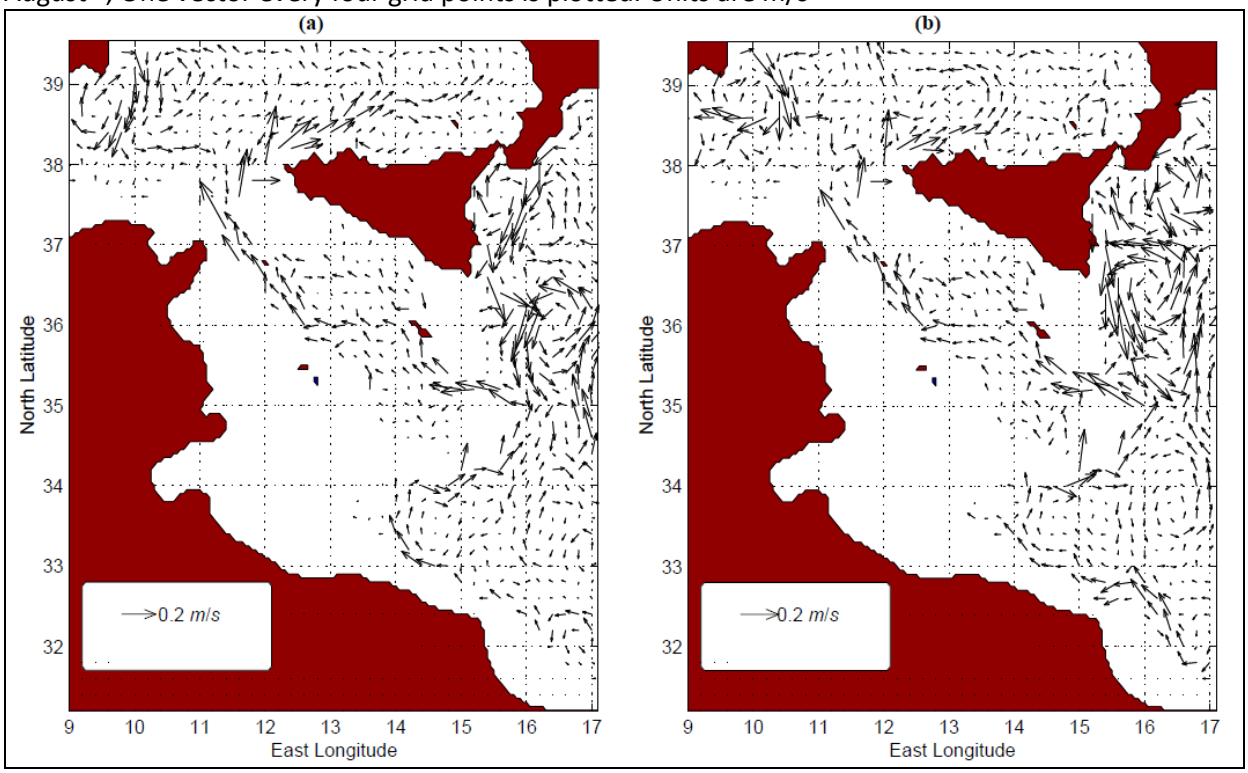

The simulated intermediate circulation at 280m (Figure 20) replicates well the westward LIW flow. The variability of the LIW is limited mainly to the intensity of the flow rather than to its spatial location.

The variability of simulated currents is investigated by Drago *et al.* (2003)[53] by means of vertical sections of the latitudinal and meridional components of the total velocity (example plots for January and October in Figure 21). The horizontal velocities are plotted at 30m, in order to view the mean surface circulation without the effect of the Ekman contribution[54]. The section runs from south to north across the Malta Channel from the Maltese coast to Sicily along longitude 14°20′E.

[52] Sorgente, R., Drago, A. and Ribotti, A. (2003). Seasonal variability in the Central Mediterranean Sea circulation. *Annales Geophysicae*, 21, 299 - 322.

[53] Drago, A.F., Sorgente, R., and Ribotti, A. (2003). A high resolution hydrodynamical 3D model of the Malta Shelf area. In *Annales Geophysicae*, 21: 323-344 pp.

[54] Surface wind stress driving a relatively shallow upper ocean flow that transports water to the left/right and the southern/northern hemisphere

Figure 21: Vertical sections of 10-day averaged east-west total velocity components and north-south total velocity components for the second third of January (a) and (b), and for the second third of October (c) and (d)[55].

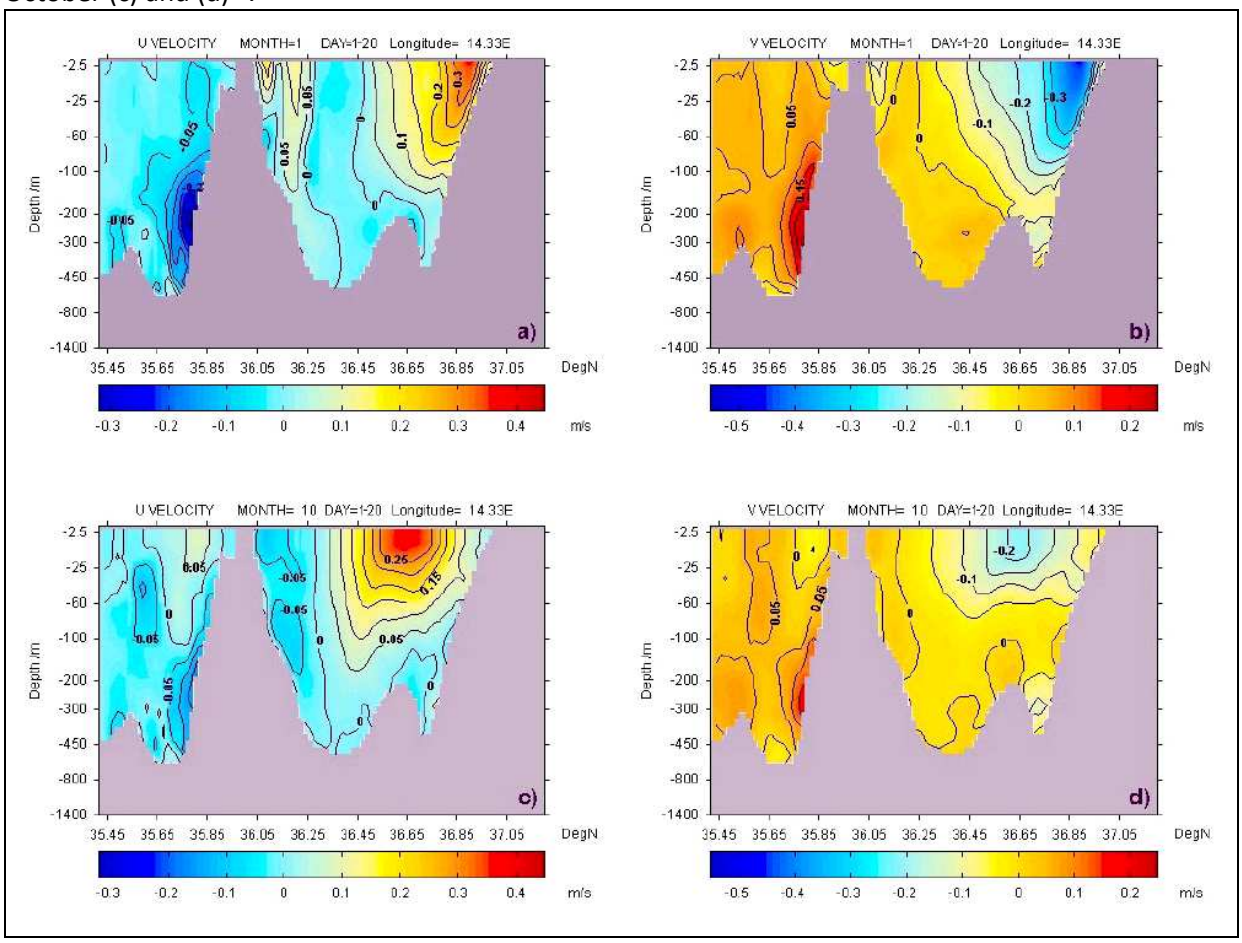

U (east-west, east positive) and V (north-south, north positive) components have been used to plot intensity and direction of the currents. In Figures (a) and (c) positive velocities are directed towards east and negative velocities directed towards west. In Figures (b) and (d) positive velocities are directed towards north and negative velocities directed towards south. They furnish a view of the vertical structure of the flow. The phenomenology and variability of the upper layer mean flow is dictated by the AIS moving eastward across the domain, and the strong upwelling activity adjacent to Sicily. The surface coastal current associated with the upwelling system flows south eastward following the Sicilian coast and merges with the AIS, forming an intense core centred over the shelf area during winter and spring. As indicated from Figure 21, the peak surface horizontal velocities reach values of around 0.4 m/s, being slightly weaker in winter. The flow has a quasi-barotropic[56] nature in the top layer, but is accompanied by strong velocity shears in the bottom boundary layer and along its lateral boundaries as it extends horizontally up to a latitude of 36.4° N, and vertically beyond the Sicilian shelf break. It practically maintains the same intensity throughout the year. In winter and spring it remains close to the coast. During summer the core velocities are slightly high, but the horizontal extent is wide and the stream practically

[55] Drago, A.F., Sorgente, R., and Ribotti, A. (2003). A high resolution hydrodynamical 3D model of the Malta Shelf area. In *Annales Geophysicae*, 21: 323-344 pp.

[56] Barotropic flow = depth-independent circulation due to changes in surface elevation

fills the whole meridional extent of the Sicilian basin and Malta platform area. Its path takes a more southward oriented diversion and tends to follow more the bathymetry. Its axis is progressively shifted southwards in late summer, culminating into a complete detachment in October; the flow is then restricted to a reduced core residing in the upper 30m and is no longer bound to the coast and bathymetry. Thus, the seasonal variability of the flow is mainly characterised by its spatial extent, position and path rather than its intensity. Inter-annual current velocities between 2008 and 2010 are depicted in Figure 22.

Figure 22: Current Velocity at 5m depth (Yearly from 2008 to 2010); Sicily Strait sub-Regional Model (SCRM)[57]

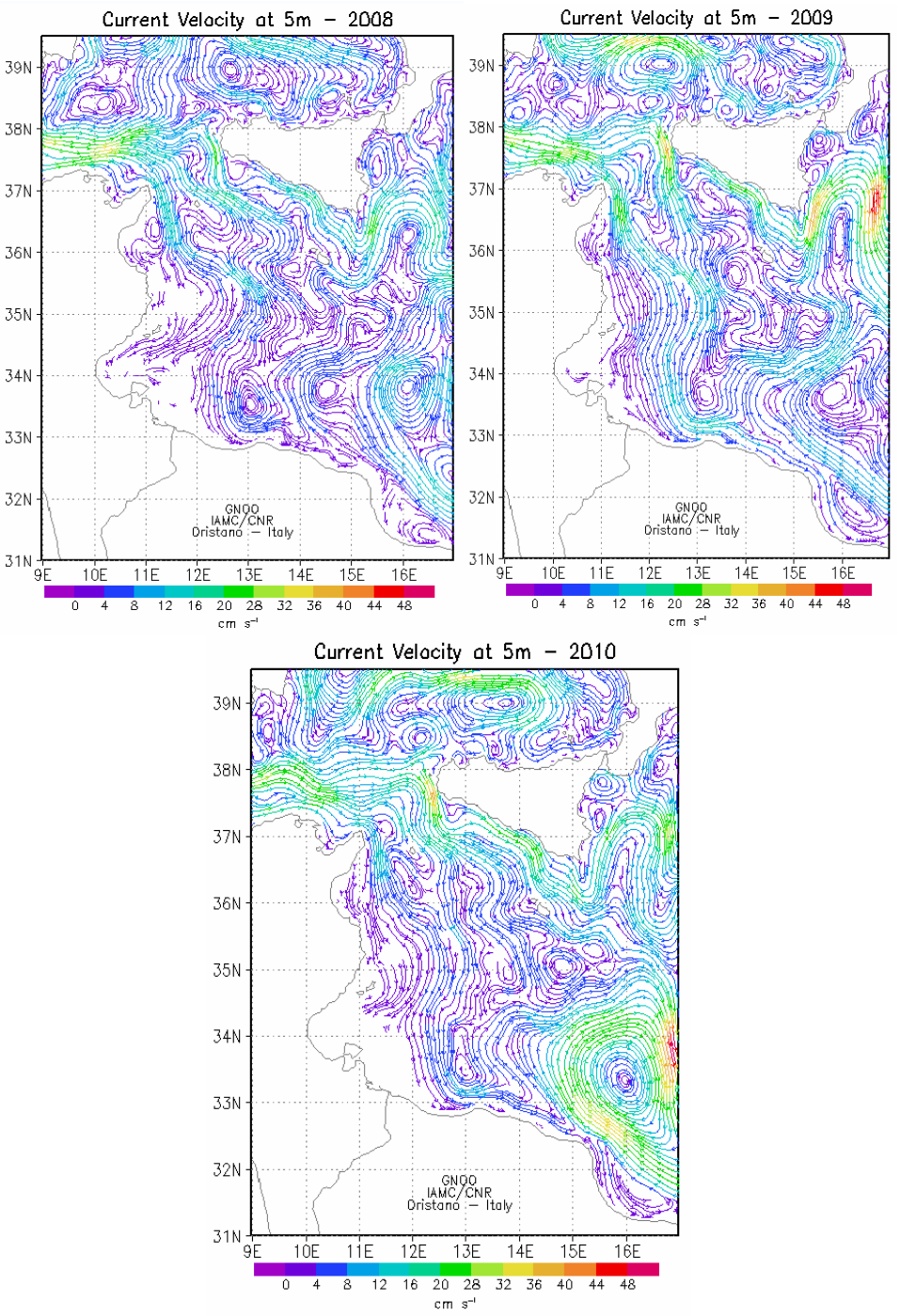

[57] Source: G30 – IAMC – CNR of Oristano - www.seaforecast.cnr.it/en/fl/sicily.php?q=4

1.6 Wave exposure

"Wind waves", that is, surface waves that occur on the free surface of oceans or seas, usually result from the wind blowing over a vast enough stretch of fluid surface. When directly being generated and affected by local winds, a wind wave system is called a "wind sea". After the wind ceases to blow, wind waves are called "swell". Wind waves differ in size/height, duration and shape, with a limited predictability. The key statistics of wind waves (both seas and swells) in evolving sea states can be predicted with numerical wind wave models, such as has been used to determine wave conditions in the sea areas around Malta. Five factors influence the formation of wind waves[58] : wind speed, distance of open water that the wind has blown over (called the "fetch"), width of area affected by fetch, time duration the wind has blown over a given area, and water depth. All of these factors work together to determine the size of wind waves.

Information on significant wave heights (SWH) and directions for the sea area up to 20 nautical miles around the Maltese Islands is documented by Scott Wilson Kirkpatrick and Co. Ltd (2003)[59] on the basis of various datasets and modelling. Initially the offshore wave/wind climate was derived and used as the basis for numerical modelling. The wave climate around the islands was then derived through model simulations, which represent all of the conditions that occur annually around Malta. The models results have been compared with available datasets to verify the output of the model. The results from the model simulations have then been analysed to determine the seas areas where the probability of exceeding significant wave heights of 1.5 and 2.5 m is less than 10%. The modelling exercise has been completed on an annual basis and for a summer period (April to October inclusive). Their findings are summarised in the following paragraphs.

This study applied UK Meteorological Office (UKMO) Wave Model data sets generated between 1988 and 2002. Wave data was obtained for 4 offshore locations (Figure 23): Point A - 14.30°E / 35.75°N (North); Point B - 14.70°E / 36.00°N (East), Point C - 14.30°E / 36.25°N (South) and Point D - 13.90°E / 36.00°N (West). Statistics for the offshore UKMO wave data are given in Table 3, for the annual and summer (April to October inclusive) periods of operation respectively.

[58] Young, I. R. (1999). Wind generated ocean waves. Elsevier. ISBN 0080433170. p. 83

[59] Scott Wilson Kirkpatrick and Co. Ltd. (2003). Malta Significant Wave Height Study, 43 p.

Figure 23: Location map for offshore wave data[60]

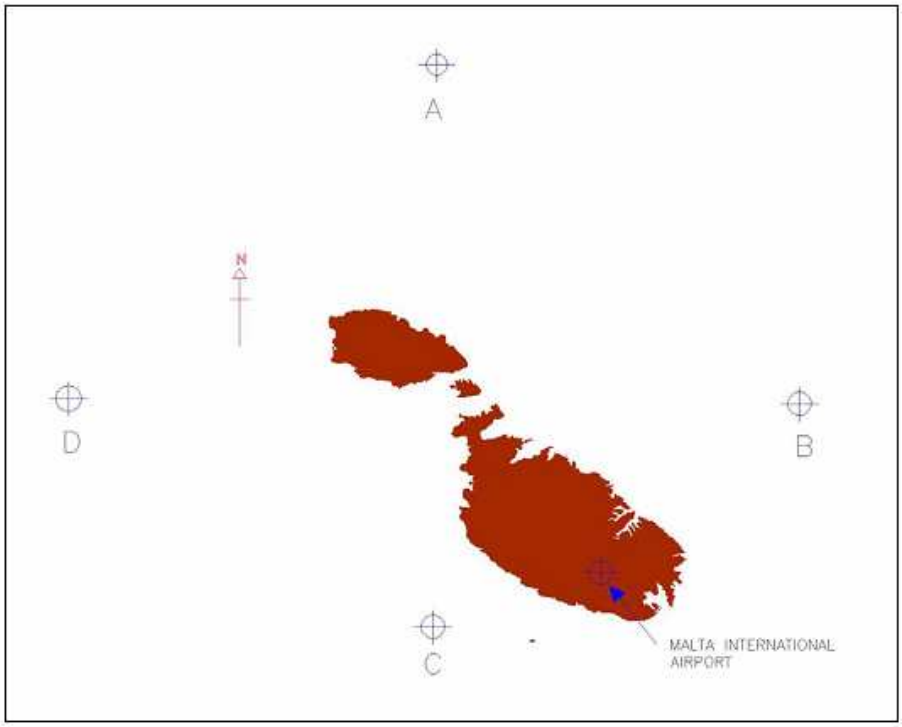

Table 3: Percentage exceedance of offshore significant wave height at Points A-D; annual and summer periods of operation

Significant Wave Height (m)	Percentage Exceedance (annual period of operation)				Percentage Exceedance (summer period of operation)			
	A	B	C	D	A	B	C	D
0	100	100	100	100	100	100	100	100
0.5	68	69	68	70	56	56	57	57
1	38	38	38	39	26	26	27	27
1.5	20	21	20	21	12	12	13	13
2	11	11	11	12	6	6	6	6
2.5	6	6	6	6	3	2	3	3
3	3	3	3	3	1	1	1	1
3.5	1	1	1	2	0	0	0	0
4	1	1	1	1				
4.5	0	0	0	0				

[60] Scott Wilson Kirkpatrick and Co. Ltd. (2003). Malta Significant Wave Height Study, 43 p.

Waves in a given area typically have a range of heights. For weather reporting and for scientific analysis of wind wave statistics, their characteristic height over a period of time is usually expressed as significant wave height (SWH). Significant wave heights are milder for the summer period when compared to the annual period of operation (Table 1). The offshore significant wave height that is exceeded for less than 10% of the time is around 2.1m annually and 1.75m for the summer period of operation. Significant wave height roses for the annual and summer periods of operation are given in Figure 24 respectively. From these plots it can be seen that the predominant wave direction is from the north-west. Waves from the south-east are also relatively frequent but waves with directions from the south-east and north-east occur less frequently.

Figure 24: Offshore significant wave height rose – Point D for the annual (left) and Summer (right) period of operation[61].

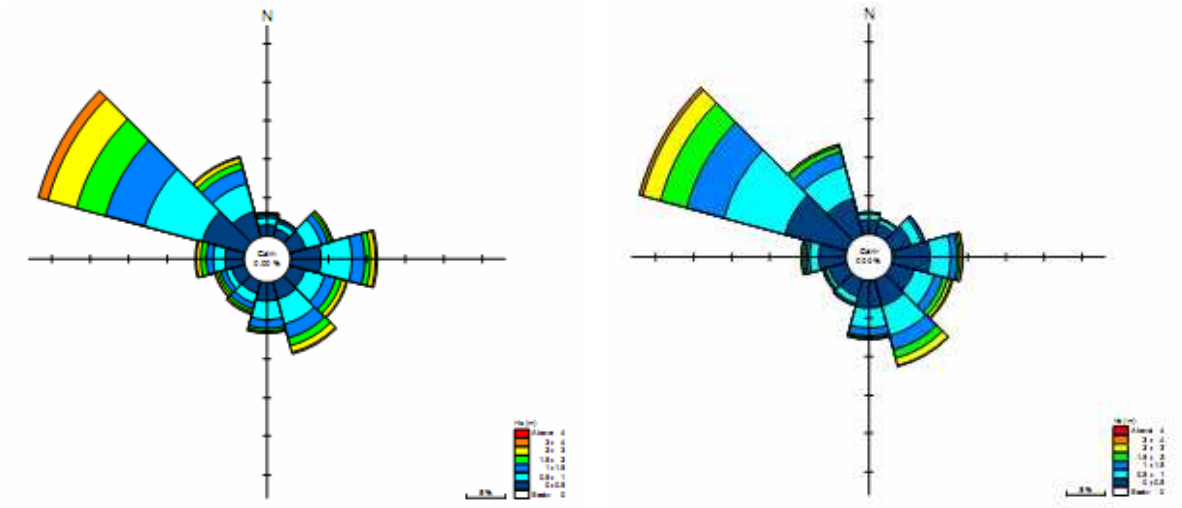

The offshore wave roses have a very similar directional distribution to the offshore wind roses. There is also a correlation between wind intensity and wave heights (Figure 25). This confirms that the wave climate around Malta is dominated by sea waves rather than swell waves. Sea waves are characterised by being steep and having relatively short wave periods when compared to swell. Sea waves are generated by the wind in the local area, whilst swell waves are waves that have been generated elsewhere and have travelled into the local area.

[61] Source: UKMO European Wave Model

Figure 25: Monthly wave (left) and wind (right) statistics[62]

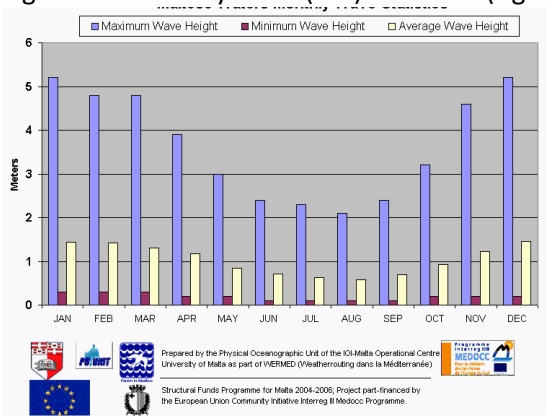

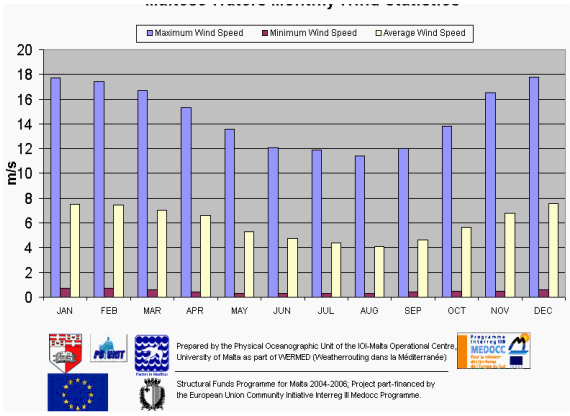

The distribution of significant wave heights show that August is the mildest month in terms of wave climate with over 60% of wave heights being in the lowest wave height band of 0 - 0.5 m. The wave height distribution for June and July is similar to that of August. The wave conditions in May are similar to those in September. In general the wave conditions are slowly varying throughout the year (cf. average values), which means that results for the summer period of operation would not be significantly affected by small changes in the start or end dates of the summer period.

The Coastal Management Company recorded wave conditions in the vicinity of Hurd Bank between 1992 and 1994[63]. The significant wave height exceeded for less than 10% of the time is approximately 2.4m annually and 1.9m for the summer period of operation. The two wave data sets, recorded by the CMC buoy and extracted from the UKMO model, are comparable. The similarity of the CMC and UKMO wave datasets supports the selected approach of using the UKMO wave model as the base dataset for the numerical modelling which has been used to determine detailed wave conditions in sea areas close to Malta.

<u>Determination of the local sea areas where the probability of exceeding 1.5 and 2.5m SWH is smaller than 10%</u>

As the Maltese Islands are not represented in the UKMO European Wave Model, a detailed numerical model has been developed for the area around Malta and Gozo using the Mike Zero Nearshore Spectral Wave (NSW) model, a nearshore modelling package developed by Danish Hydraulic Institute (DHI). Contoured 10 percentile values of SWH have been determined at 0.5m intervals from 1.5m and above. Two maps have been produced: annual climate and summer climate (Figure 26).

[62] Source: PO Unit – IOI Malta Operational centre

[63] Coastal Management Company Ltd (1995) Wave Data Statistics from Offshore Wave Monitoring Buoy 1992-1994. Report GC 9502 prepared for Gozo Channel Co. Ltd. May 1995.

Figure 26: Sea areas where the Significant Wave Height is exceeded for 10% of the year (left) and Summer period of operation (right)[64].

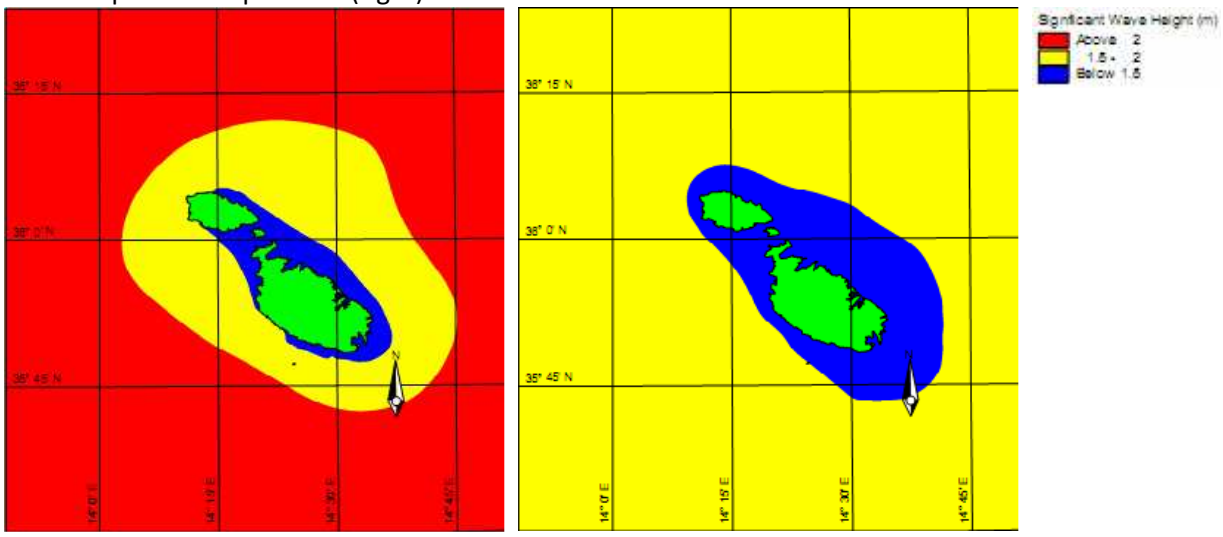

For the annual period of operation and for the wider sea area around Malta, the significant wave height that is exceeded for 10% of the year is between 2.0 and 2.5m. The significant wave height that is exceeded for 10% of the year is between 1.5 and 2.0m for a sea area that extends approximately 20km offshore to the north-east of the islands and 10km to the south-west. The sea area where the 10%ile exceedance significant wave height does not exceed 1.5m does not extend all the way around the islands. To the north of the islands the sea area extends out to about 5km from the coastline. There are two coastal areas where the 10%ile exceedance significant wave height exceeds 1.5m: (1) to the north-west of Gozo and (2) to the south of Malta. The main sea routes between Malta, Comino and Gozo all fall within the lowest specified significant wave height band (<1.5m). For the summer period of operation and for the wider sea area around Malta, the significant wave height that is exceeded for 10% of the period is between 1.5 and 2.0m. The sea area for the lowest specified significant wave height band (1.5m) extends all the way around the islands. The significant wave height that is exceeded for 10% of the year is between 0 and 1.5 for a sea area that extends approximately 10km offshore to the north-east of the islands and less than 5km to the south-west. It should be noted that the two maps show the 10%ile significant wave height for the sea areas in which vessels operate, and are not intended to represent conditions caused by localised effects such as reflection from breakwaters. Comparisons between the NSW model and available results from previous studies have been made; in summary, there is reasonable agreement between the different predictions.

Determination of the wave energy density

The following wave climatologies (Figure 27) are based on a database consisting of a 44-year (1958 – 2001) dataset of wind and wave hourly values at a horizontal resolution of 0.125 degrees on the domain covering the area of interest over the Central Mediterranean area. Other parameters like wave height and direction, peak wave period and mean wave period can also be viewed on: http://www.capemalta.net/maria/pages/climatologies.html

[64] Source: Scott Wilson Kirkpatrick and Co. Ltd. (2003). Malta Significant Wave Height Study, 43 p.

Figure 27: Seasonal average wave energy density in the Central Mediterranean Sea[65]

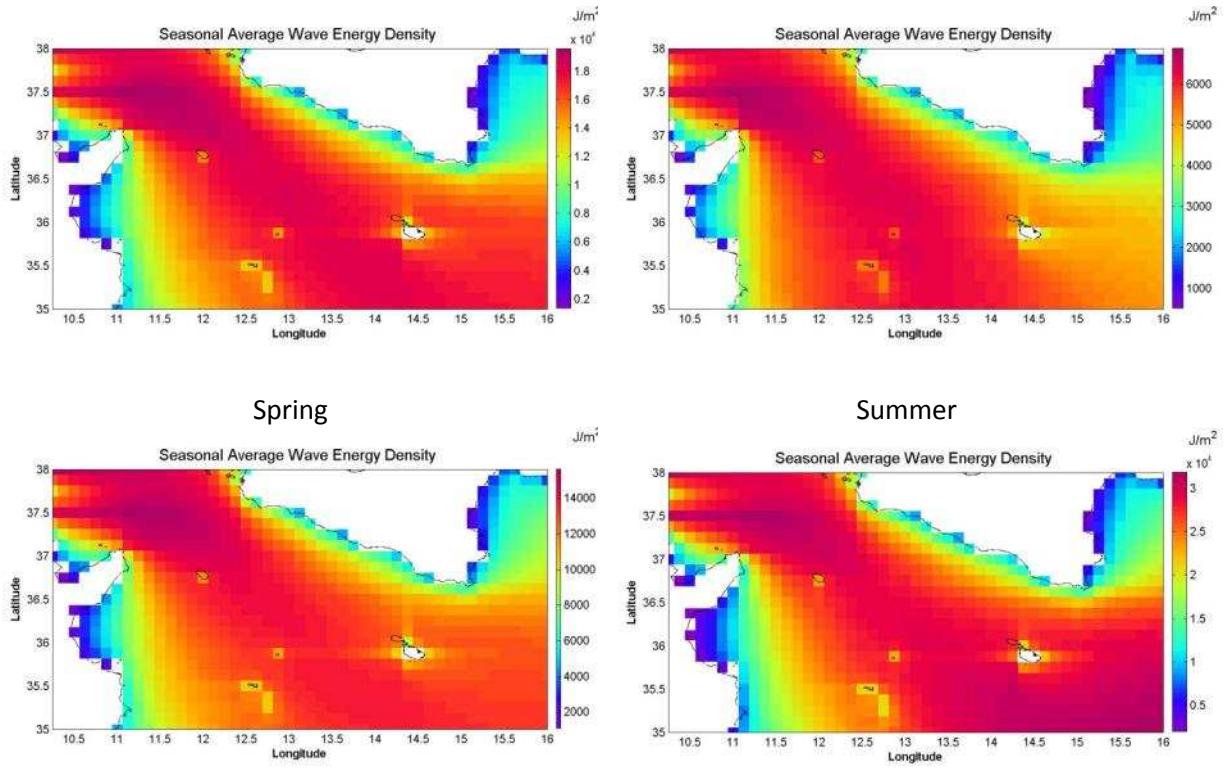

As for the wave height, the energy of waves progressively increases from summer to winter. Values are more important than in the Tunisian east coast and South of Sicily, because of the position of Malta in the middle of Central Mediterranean Sea.

Daily predictions of sea state conditions around the Maltese Islands

The Maria Malta Wave forecasting system provides daily predictions of sea state conditions in the Central Mediterranean and the area around the Maltese Islands. The operational setup produces wave forecasts at the level of the entire Mediterranean region at a resolution of 0.5° in both longitude and latitude, as well as at a higher resolution of 0.125° covering the central Mediterranean. The output parameters from the model are: significant wave height, mean wave direction and frequency of total sea, wind waves and swell (example with wave height and direction: Figure 28). Forecasts may be viewed on: http://www.capemalta.net/maria/pages/waveforecast.html

[65] www.capemalta.net

Figure 28: Sample Output from the Malta Maria Wave Forecast system (Wave height and direction - Central Mediterranean Sea - 17th of April 2012, 21h GMT)[66].

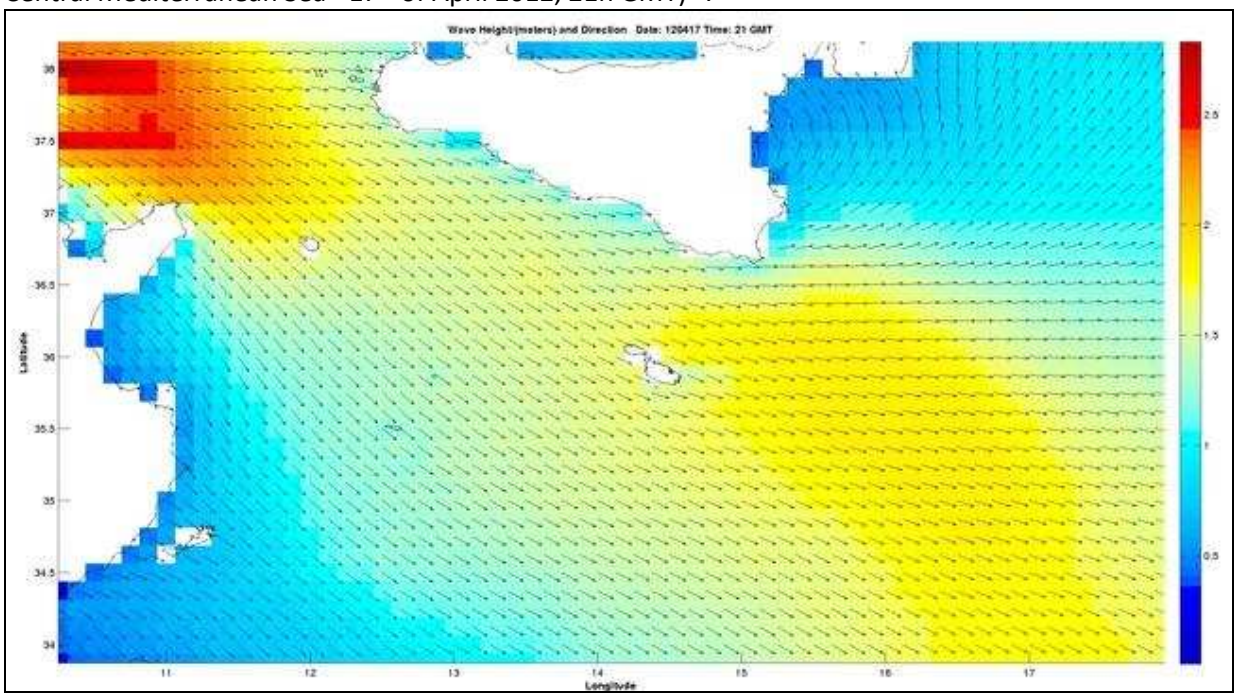

1.7 Upwelling

Upwelling is a process that can occur in the open ocean and along coastlines and results in deeper water rising to the surface to replace water that is pushed away by wind blowing across the ocean surface. Water that rises to the surface as a result of upwelling is typically colder and is rich in nutrients. Frequent coastal upwelling events occur along the westward and southern coast of Sicily. Such upwelling is induced by westerly winds and by inertia of the isopycnal domes of the AIS meanders and cyclonic vortices. The upwelling in this area is relevant in an ecological sense because of the implications in the population dynamics of some commercially important small pelagic fishes. Due to the presence of large mesoscale phenomena in the Straits of Sicily, the upwelling can extend its influence far offshore, as documented by infrared satellite observation (refer to Figure 29). The south-eastward advection of these cold patches in the form of long plumes and filaments are a very characteristic feature in the thermal IR images of the region.

[66] www.capemalta.net

Figure 29: Upwelling along the Southern coast of Sicily triggered by strong NW winds (2002)[67]

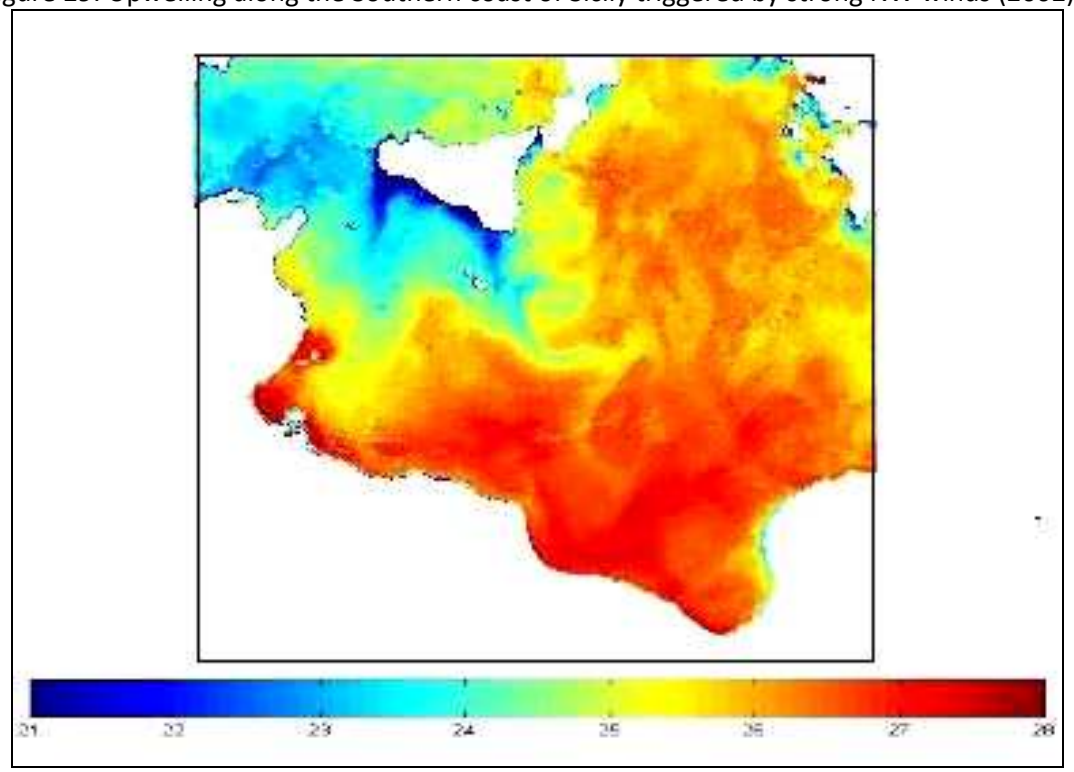

As seen in Figure 29, the upwelling zone runs along the whole southern coast of Sicily and extends for a considerable distance (about 100 km) offshore, especially over the Adventure Bank and on the Malta platform. The inclination of the isotherms (not shown) indicates that upwelling persists from May to December, being most evident in the summer months and early fall when the water column becomes well stratified and the thermocline is able to surface close to the southern Sicilian coast.

The thermal signature of the upwelling is more evident in the climatological maps (Figure 30) in summer and autumn (bottom panels) than in winter and spring (upper panels), due to the stronger contrast between upwelled waters and the upper, warm stratified layer. In summer the upwelling is probably enhanced by the action of the AIS.

[67] Source: Drago, A., Sorgente, R., and Olita, A. 2010. Sea temperature, salinity and total velocity climatological fields for the south-central Mediterranean Sea. GCP/RER/010/ITA/MSM-TD-14. *MedSudMed Technical Documents*, 14: 35 pp.

Figure 30: Temperature map at 30 m depth for (left-right and top-bottom) winter, spring, summer and autumn[68]

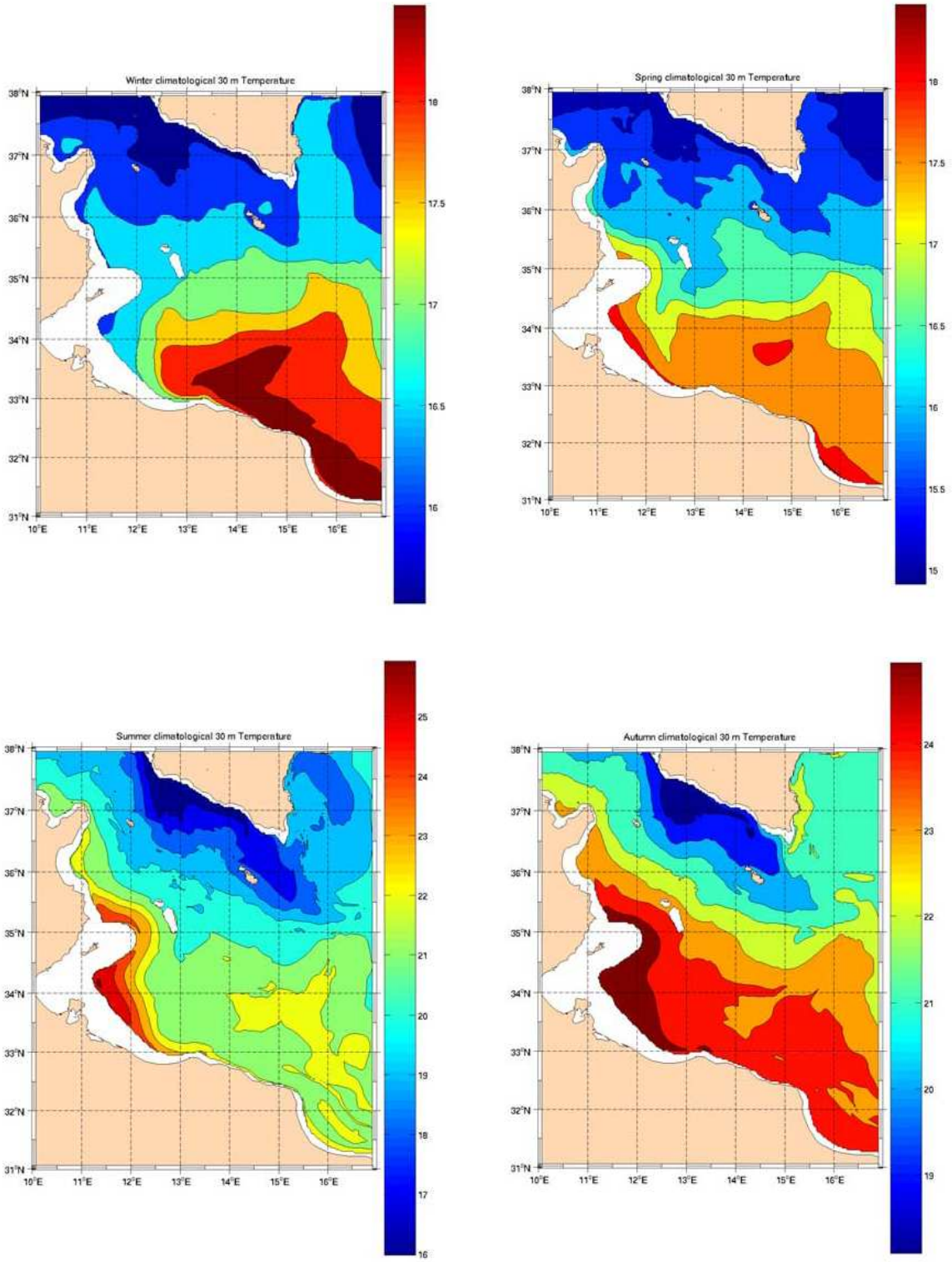

[68] Source: Drago, A., Sorgente, R., and Olita, A. 2010. Sea temperature, salinity and total velocity climatological fields for the south-central Mediterranean Sea. GCP/RER/010/ITA/MSM-TD-14. *MedSudMed Technical Documents*, 14: 35 pp.

1.8 Transparency and Turbidity – Characteristics and Trends

Prior to 2005, the bathing water quality monitoring programmes comprised taking measurements of transparency and turbidity in coastal bathing waters. Water transparency was initially measured using a Secchi discs and only recently was it measured *in situ* by means of a submersible transmissometer and reported in terms of beam attenuation coefficients (BAC) at 660nm. For a monochromatic beam travelling through a water column containing suspended particles, light loss is either by absorption into other forms of energy, or by scatter outside of the collimated beam. The amount of light loss depends upon the length of water column (25cm in this case) and the coefficients of light absorption and light scatter by the particles suspended in the water. The beam attenuation coefficient includes both absorption and light scatter losses. Clear offshore waters usually have beam attenuation coefficients below $0.18m^{-1}$ while turbid waters under the influence of land-based discharges tend to have values above $1m^{-1}$. Figure 31 shows on the basis of results obtained by Axiaq (2004)[69] the trend between 1998 and 2004 for the mean levels of water turbidity as expressed in BAC, relative to reference sites (percentages) for different coastal areas subjected to specific pressures. Trends for this period under review are complex to interpret in view of the significant natural fluctuations of the same water quality parameter in reference sites. Nonetheless, it is evident that for port areas, (including Marsa Creek under the influence of the power station), there was a persistent upward trend in water turbidity. For the period 1998 to 2004, water turbidity was found to be the highest in those areas exposed to discharges by power stations. Port areas and areas in the vicinity of sewage outfalls also exhibited increased water turbidity with respect to reference sites. It should be noted that all untreated sewage outfalls have been replaced by treated sewage effluents (since 2011). Areas exposed to fish farms exhibited only marginally increased water turbidity. Water transparencies in terms of Secchi depths in the various different coastal zones showed the same tendencies as those identified above for BAC valued.

[69] Axiaq, V. (2004) Marine Coastal Monitoring Programme: June 2003, March 2004

Figure 31: Mean water turbidity (BAC) in various coastal zones under different anthropogenic influences, relative to reference sites[70]

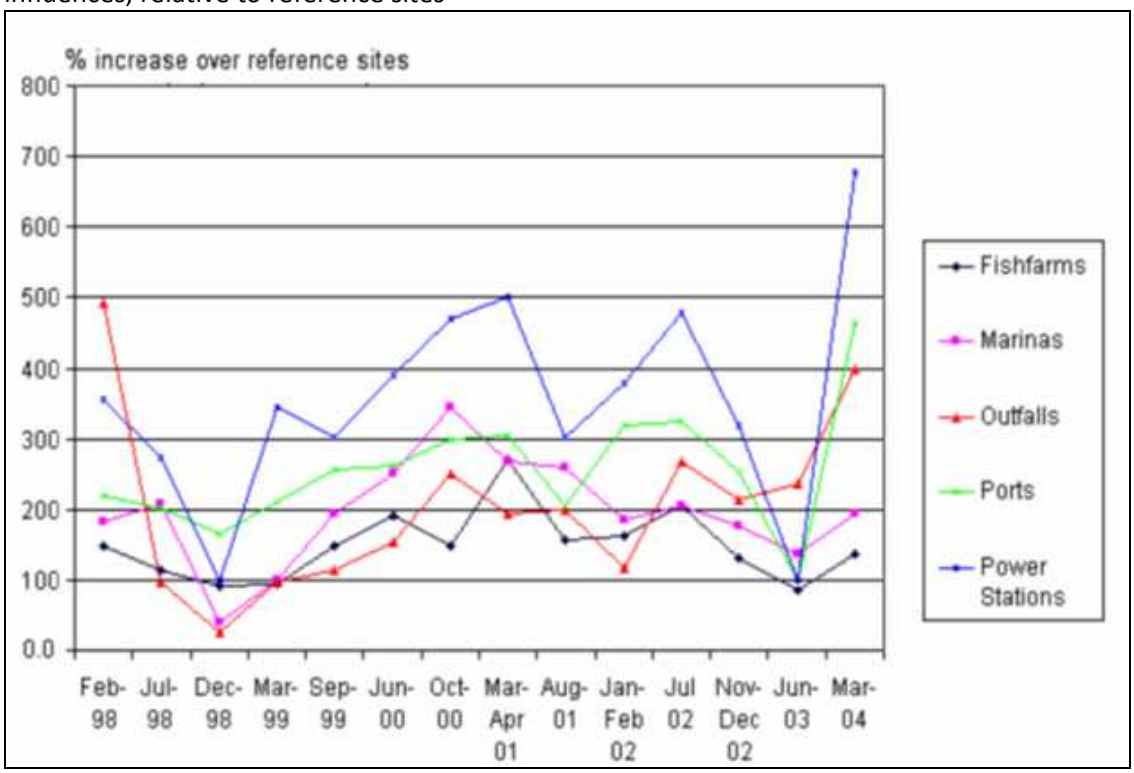

Sea turbidity is also one of the physicochemical parameters that are monitored in compliance with the Water Framework Directive. The method employed is APAT CNR IRSA 2110 Man 29 2003. Turbidity readings (in Nephelometric Turbidity Unit) are shown in Table 4 and Figure 32 for the year 2012. None of the readings exceed 5NTU.

[70] Axiaq, V. (2004) Marine Coastal Monitoring Programme: June 2003, March 2004

Table 4: Turbidity readings at 5m depth using a multi-parametric probe (means and SD)[71]

2012						
Monitoring Position	**1st Survey 29 May to 6 June**	**2nd Survey 27 June and 2-3 July**	**3rd Survey Beginning of August**	**4th Survey End Aug/ Beginning Sep**	**5th Survey End Sep/ Beginning Oct**	**6th Survey End Oct/ Beginning Nov**
CN01-1		3.5± 0.14 2 July	4.1± 0.14 1 Aug	3.9± 0 29 Aug	3.85±0.07 5 Oct	3.7±0.141 26 Oct
CN01-2	3.6± 0.0 30 May	3.6± 0.0 2 July	3.8± 0.28 1 Aug	3.9± 0 29 Aug	4.05±0.07 5 Oct	3.8±0.00 26 Oct
CN02-1		3.6± 0.0 2 July	3.6± 0.28 1 Aug	3.9± 0 29 Aug	4.10±0.00 5 Oct	4.2±0.141 26 Oct
CN03-1	3.6± 0.0 30 May		3.6± 0.28 2 Aug	3.95± 0.07 29 Aug	3.79±0.01 28 Sep	3.7±0.141 26 Oct
CN03-2		4.6± 0.99 2 July	3.8± 0.28 2 Aug	4.4± 0.14 29 Aug	4.1±0.00 28 Sep	3.8±0.00 26 Oct
CN04-1	3.6± 0.0 31 May	3.6± 0.14 27 June	3.9± 0.57 3 Aug	3.95± 0.07 29 Aug	3.85±0.07 28 Sep	3.3±0.141 26 Oct
CN04-2		3.6± 0.0 27 June	3.3± 0.14 7 Aug	3.95± 0.07 30 Aug	4.30±0.00 6 Oct	3.55±0.0707 26 Oct
CN04-4		3.7± 0.14 27 June	4± 0.28 3 Aug	4± 0.00 30 Aug	4.05±0.07 6 Oct	3.5±0.00 26 Oct
CN04-5		3.7± 0.28 27 June	4.6± 0.14 6 Aug	4.1± 0.14 30 Aug	4.10±0.00 6 Oct	3.3±0.00 26 Oct
CN04-6		3.7± 0.14 27 June	4.2± 0.14 6 Aug	3.95± 0.07 30 Aug	4.25±0.07 6 Oct	3.6±0.141 26 Oct
CN05-1	3.7± 0.14 4 June	4.2± 0.28 27 June	3.7± 0.0 6 Aug	3.85± 0.07 30 Aug	3.70±0.00 6 Oct	3.8±0.00 26 Oct
CN06-1		4.2± 0.57 3 July	37.6± 0.28 6 Aug	4.05± 0.07 30 Aug	4.00±0.14 6 Oct	3.9±0.141 4 Nov
CN07-1	3.7± 0.14 2 June	3.6± 0.14 3 July	4.3± 0.14 6 Aug	4± 0.00 30 Aug	4.15±0.07 6 Oct	3.85±0.070 4 Nov
CN07-2		3.7± 0.28 3 July	4.3± 0.42 5 Aug	3.95± 0.07 30 Aug	4.15±0.21 6 Oct	3.95±0.212 4 Nov
CN07-3		4.3± 0.71 3 July	4.5± 0.28 5 Aug	4.35± 0.07 30 Aug	4.00±0.14 6 Oct	4±0.141 4 Nov
CN09-1		3.5± 0.14 2 July	4.1± 0.28 2 Aug	4± 0.00 29 Aug	4.05±0.07 28 Sep	3.35±0.353 26 Oct
CP04-1	3.5± 0.14 31 May	3.6± 0.0 27 June	4.6± 0.28 6 Aug	3.9± 0.00 30 Aug	4.20±0.00 6 Oct	3.6±0.00 26 Oct
CP04-2		3.6± 0.0 27 June	3.6± 0.42 7 Aug	4± 0.00 30 Aug	3.85±0.07 6 Oct	3.3±0.141 26 Oct
CP05		3.8± 0.28 3 July	4± 0.14 6 Aug	3.95± 0.07 30 Aug	4.00±0.14 6 Oct	3.4±0.00 26 Oct
CP06-1	3.6± 0.0 4 June	3.6± 0.0 3 July	3.6± 0.14 6 Aug	3.9± 0.00 30 Aug	4.25±0.07 6 Oct	3.95±0.070 4 Nov
CP07	3.9± 0.14 2 June	3.6± 0.0 3 July	3.9± 0.28 5 Aug	3.9± 0.00 30 Aug	4.20±0.00 6 Oct	3.75±0.212 4 Nov
CS01		3.5± 0.0 2 July	4± 0.14 1 Aug	3.95± 0.07 29 Aug	3.85±0.07 5 Oct	3.75±0.070 26 Oct
CS02	3.6± 0.0 30 May	3.5± 0.14 2 July	3.7± 0.0 1 Aug	3.95± 0.07 29 Aug	3.75±0.07 5 Oct	4.2±0.141 26 Oct
CS03	3.6± 0.0 6 June	3.5± 0.14 2 July	3.5± 0.14 3 Aug	4± 0.00 29 Aug	3.9±0.00 28 Sep	3.7±0.424 26 Oct
CS08		3.5± 0.14 3 July	3.9± 0.57 5 Aug	4.05± 0.07 30 Aug	4.25±0.07 6 Oct	3.7±0.141 4 Nov
CS09	3.6± 0.0 2 June	3.4± 0.14 2 July	4.4± 0.42 2 Aug	4± 0.00 29 Aug	3.7±0.00 28 Sep	3.45±0.212 26 Oct

[71] CIBM and Ambiente SC (2013) Development of Environmental Monitoring Strategy and Environmental Monitoring Baseline Surveys – Water Lot 3 – Surveys of Coastal Water – November 2012. ERDF156 - Developing national environmental monitoring infrastructure and capacity

Figure 32: Turbidity (NTU) between May and November for the Year 2012